Mon. Not. R. astr. Soc. (1977) **180**, 343–371

Radiation from relativistic blast waves in quasars and active galactic nuclei

R. D. Blandford* *Institute of Astronomy, Madingley Road, Cambridge CB3 0HA*

C. F. McKee *Departments of Physics and Astronomy, University of California, Berkeley, California, USA*

Received 1977 February 2; in original form 1976 December 13

Summary. An analysis is presented of the synchrotron and inverse Compton radiation that would be observed from behind a strong, relativistic, spherical shock propagating outwards through an ionized, magnetized medium. It is shown that, under a wide variety of conditions, a large fraction of the total dynamical energy can be dissipated in this manner. Details of the observed spectrum and its variation with time are computed for a selection of simple assumptions about the nature of the initial explosion, the ambient external medium and the relativistic particle spectrum.

It is proposed that the rapidly variable, non-thermal emission observed from many types of active galactic nucleus originate in this manner, thus avoiding the well-known Compton problem. Illustrative applications of the analysis are made to 3C120, CTA102 (in which the low-frequency variability can only be explained if the surrounding medium is inhomogeneous), AO 0235+164 and Centaurus A.

1 Introduction

The nature of quasars and active galactic nuclei is probably most clearly revealed by the rapid large amplitude fluctuations in their emitted radiation. Radio variation has been observed on timescales of days to years with powers $\sim 10^{40}$–10^{45} erg/s. Variations in optical output can be even faster and have luminosities up to 10^{48} erg/s (e.g. Rieke *et al.* 1976). X-ray variability has been observed in the nucleus of the radio galaxy Centaurus A (Winkler & White 1975) with a timescale ~ 1 week.

The most detailed variability data are at radio wavelengths, and the earliest observations were consistent with a simple, uniformly expanding spherical model (Shklovsky 1960; Pauliny-Toth & Kellermann 1966; van der Laan 1966) in which the magnetic field varies as $B \propto R^{-2}$, with R the radius, and the electrons lose energy adiabatically, $E \propto R^{-1}$. At sufficiently low frequencies, the source becomes optically thick due to self-absorption as is indeed observed. Despite its initial success, several problems remain with this interpretation.

* Present address; W. K. Kellogg Radiation Laboratory, 130–33, Caltech, Pasadena, California 91125, USA.

On the theoretical side, the model is clearly incomplete as it does not include any dynamics, which makes it impossible to estimate the total energy associated with each outburst. Furthermore, in several radio sources the upper limits to the angular size, estimated on the basis of the timescales of variability assuming non-relativistic expansion, are noticeably smaller than those measured directly by *VLBI*. In addition if the radiation energy density within these sources exceeds the field energy density then inverse Compton scattering by the relativistic electrons becomes important. This can greatly increase the total energy requirement of the source and may even lead to contradictions with observational limits at higher frequencies. These problems have been reviewed by Burbidge, Jones & O'Dell 1974, hereafter BJO). It was originally pointed out by Rees (1966) that some of these difficulties may be alleviated if the sources expand relativistically. *VLB* observations (e.g. Cohen 1975), which are often most simply interpreted in terms of relativistic kinematic effects, support this suggestion but the source energetics still depend on a detailed model. At infrared and optical wavelengths, the inverse Compton problem is possibly even more severe (Hoyle, Burbidge & Sargent 1966) and there is an additional difficulty because the anticipated electron cooling lengths are typically much less than the size of the source.

In this paper we describe an idealized model intended to account for all non-thermal variability in galactic nuclei and based on an analysis of relativistic blast waves (Blandford & McKee 1976; Paper I). Some of these ideas have been discussed independently by Jones & Tobin (1977), while an alternative dynamical approach has been followed by Vitello & Pacini (1976, preprint) in their investigation of freely expanding radio sources. We propose that as a result of an explosion or instability within a central compact object, an expanding shock wave (possibly relativistic) provides a continuous source of relativistic electrons capable of synchrotron and inverse Compton radiation. We believe that this interpretation is superior to most existing models for four main reasons. Firstly, it is dynamically self-consistent and involves relativistic motion for which we have direct observational evidence. Secondly, the particle acceleration is local, i.e. it can occur simultaneously over the emitting volume and thus avoid both serious adiabatic and radiative losses and the inverse Compton problem which, while generally mild at radio wavelengths, can be very serious in the optical region of the spectrum. Thirdly, the particle acceleration process we postulate – the dissipation of a fraction of ordered kinetic energy behind an expanding shock front – is a mechanism that we can clearly see occurring outside the solar system, namely in radio supernova remnants. Finally, as we demonstrate below, it is usually possible to develop a model for a specific nonthermal outburst that is highly efficient in the sense that the total energy inferred to be associated with the outburst exceeds that directly observed in the form of radiation by less than a factor ten. In some previous calculations using different assumptions, this factor exceeds a million and is probably incompatible with the cosmological interpretation of quasar redshifts. As we show below, this high efficiency is partly due to the fact that the mean electron energy expected behind the shock is comparable with that required to account for the nonthermal emission. This is in contrast to supernova remnants for which their ratio exceeds a thousand.

In Section 2 we give a treatment of the physical processes occurring behind the shock and in Section 3 we apply these calculations to the observations of variable radio sources. In Section 4 we continue with a discussion of the optical observations. Possible implications of these ideas for observational and theoretical studies of active galactic nuclei are described in Section 5.

These interpretations are obviously dependent on the precise details of the physical model. As far as possible, we have tried to parameterize our uncertainty by a series of dimensionless constants, k_x, all of order unity. These are listed in Table 6. Many of these can be calculated in non-relativistic and extreme relativistic limits as shown in the Appendix. How-

ever, in order to understand the basic physics within Section 2, these constants can usually be set equal to unity. A list of physical variables introduced in the text is to be found in Table 5 (see Appendix).

2 Physics of blast waves

2.1 DYNAMICS

The release of a large amount of energy in a small volume produces a shock wave which expands into the surrounding medium. The case in which the energy release is impulsive and the resulting expansion is non-relativistic (NR) and spherically symmetric is conventionally adopted as a description of the evolution of supernova remanents (Woltjer 1972). The case of steady injection of energy has been proposed as a model for the evolution of H II regions around stars with strong winds (Castor, McCray & Weaver 1975).

Extreme relativistic (ER) spherically-symmetric blast waves were analysed in Paper I. If the external density varies as a power of the radius, $\rho_1 \propto r^{-k}$, and energy is injected either impulsively or as a power of the time, then a similarity solution can be obtained by taking the shock Lorentz factor Γ to also vary as a power of the time, $\Gamma^2 \propto t^{-m}$. (Restrictions on the values of k and m are discussed in Paper I.) In contrast to the non-relativistic case, both the energy and the momentum are concentrated in a thin shell of thickness $\sim R/\Gamma^2$. Each part of the shell expands approximately independently of the rest of the shell, and this facilitates extension of the analysis to the non-spherical case, which is discussed qualitatively in Section 5.

As shown in Paper I, the dynamics of both NR and ER blast waves are governed by the equations

$$E = k_\sigma w_1 \Gamma^2 \beta^2 V \qquad \text{(AI)} \qquad (1)$$

$$L_1 t = k_\sigma w_1 \Gamma^4 \beta^2 V \qquad \text{(SI)} \qquad (2)$$

where $V = \frac{4}{3}\pi R^3$ is the volume swept out by the shock, $\beta = (1 - \Gamma^{-2})^{1/2}$ is the shock velocity in units of c, w_1 is the relativistic enthalpy ahead of the shock and k_σ ($\equiv \sigma$ in Paper I) is a numerical constant of order unity depending on the nature of the external medium and of the shock (see Table 7). Here E is the energy of the adiabatic impulsive (AI) explosion. The luminosity of the central power supply in the steady injection (SI) case is L_1; the shock can be either adiabatic or radiative. We assume that the internal fluid constituting the piston in the SI case is ultrarelativistic ($\kappa(\hat{\gamma}_i) = 1$ in the notation of Paper I). We use the term 'radiative shock' to mean one in which the electron energy is radiated away. In contrast to our assumption in Paper I, it is not necessary that the ion internal energy be radiated as well. The energies of the ions and electrons should be well coupled in the highly turbulent shock front, but behind the shock there is probably no effective mechanism to transfer ion energy to the electrons unless the densities are much higher than those appropriate to active galactic nuclei. In this case radiative losses have a smaller effect on the dynamics of SI shocks than found in Paper I; radiative impulsive shocks in which only the electrons radiate will rapidly decelerate and must be considered separately, but we do not discuss them here. Of course if the external medium is composed mainly of electrons and positrons, then all the internal energy can be radiated away and the shock is radiative in the sense of Paper I as well.

Two additional assumptions were made in obtaining the above equations. First, the shock is assumed to be strong in the sense that the random kinetic energy per particle ($\propto p'/n'$, where p' is the pressure and n' the electron density) behind the shock is much greater than

that ahead. If the ratio of specific heats of the gas ahead of and behind the shock is 4/3, this assumption requires

$$\gamma_2 - 1 \gg \tfrac{3}{4}(1 - 1/k_w), \tag{3}$$

where γ_2 is the bulk Lorentz factor of the gas just behind the shock as measured in the fixed frame and k_w is the ratio of the particle enthalpy to the rest energy density, $\rho_1 c^2$ ahead of the shock, $k_w \equiv w_1/\rho_1 c^2 \geqslant 1$. Even if the external medium is extremely relativistic ($k_w \gg 1$), this is not a very stringent limitation on the shock Lorentz factor, $\Gamma \simeq 2^{1/2}\gamma_2$.

The second assumption is that the magnetic field is too weak to affect the dynamics. The relative importance of the external magnetic field, B_1, is measured by the parameter

$$b = \frac{\rho_1 c^2}{(B_1^2/8\pi)}. \tag{4}$$

The requirement that the magnetic pressure behind the shock be less than the gas pressure implies

$$b > \frac{2(5\gamma_2 + 4)}{\gamma_2 k_w - 1} \equiv b_{\rm mag}, \tag{5}$$

where for simplicity we have taken B_1 normal to the shock velocity and have assumed the ratio of specific heats of the shocked gas to be 4/3. By comparison, the equipartition field strength, defined by equating the post-shock internal and magnetic energy densities, corresponds to $b_{\rm eq} \sim \tfrac{1}{3} b_{\rm mag}$. Hence our analysis is strictly restricted to field strengths in the shocked fluid significantly less than the equipartition value.

Integration of equations (1) and (2) shows that the shock radius R can be expressed

$$R = k_R \beta c t, \tag{6}$$

where $k_R = 1$ in the ER case and is listed for several non-relativistic cases in Table 1. Note that $R \propto t^{1/k_R}$. An Earth-bound observer describes the expansion in terms of the time, t_0, at which signals arrive at Earth

$$R = k_0 \Gamma^2 \beta c t_0 \tag{7}$$

(see Appendix). In terms of t_0 we have $\Gamma^2 \propto t_0^{-m/(m+1)}$ and $n_1 \propto R^{-k} \propto t_0^{-k/k_R(m+1)}$. Since t is measured at the source and t_0 at Earth, the constant k_0 depends on the redshift z through the factor $(1+z)^{-1}$ (Table 6). For a relativistically expanding sphere, only part of the sphere is visible and the measured angular radius is

$$\theta = k_\theta R/\Gamma D, \tag{8}$$

Table 1. Shock dynamics: values of m, k_R.

Energy supply	External medium	Shock velocity	m	k_R
Impulsive	Uniform	NR	0	5/2
	($k = 0$)	ER	3	1
	Wind	NR	0	3/2
	($k = 2$)	ER	1	1
Steady injection	Uniform	NR	0	5/3
	($k = 0$)	ER	1	1
	Wind	NR	0	1
	($k = 2$)	ER	0	1

where D is the luminosity distance of the source (calculated assuming $H_0 = 50$ km/(s Mpc), $q_0 = 0$). Where measured *VLB* sizes are available, we have used values of k_θ appropriate to expanding spheres in order to estimate the linear dimensions. This is probably not a very good approximation but little better is achievable without an improved understanding of the interpretation of *VLB* data.

2.2 PARTICLE ACCELERATION

There is a considerable uncertainty about the electron distribution function behind a rapidly moving collisionless shock. We shall assume that a specific fraction k_e of the particle kinetic energy in the frame of the shocked fluid goes into the electrons, and that the distribution function is either a Maxwellian or a power law in energy.

For shocks in which the *mean* electron Lorentz factor $\bar{\gamma}'_e$ measured in the comoving frame just behind the shock is much greater than one, the shock jump conditions imply

$$\bar{\gamma}'_e = k_e k_\gamma \Gamma\beta^2 (m/m_e) \tag{9}$$

where the prime indicates the comoving frame and m is the mean mass per electron. (In applications we shall take $m = 1.95 \times 10^{-24}$ g, corresponding to a plasma with a helium/hydrogen ratio of 0.1 by number). This equation is central to our analysis: it directly relates the energy of the electrons observed via their radiation to the dynamics of the source as a whole. The uncertainty lies in the choice of the fraction k_e and the relevant distribution function. The large-amplitude electromagnetic fields developed in the shock front probably result in approximate equipartition between electrons and ions, i.e. $k_e \sim \frac{1}{2}$, although the evidence in favour of this (McKee 1971, 1974) is far from convincing.

For a relativistic Maxwellian, the electron temperature is $\frac{1}{3}\bar{\gamma}'_e m_e c^2/K_B$, where K_B is Boltzmann's constant. If the distribution function is a power law ($dn/d\gamma'_e \propto \gamma'^{-s}_e$), we assume it extends from γ'_1 to γ'_u. The mean Lorentz factor is $\sim [(s-1)/(2-s)]\, \gamma'^{2-s}_u \gamma'^{s-1}_1$ if $1 < s < 2$; for $s > 2$, the mean Lorentz factor is $\sim [(s-1)/(s-2)]\, \gamma'_1$.

A power-law photon spectrum can arise in one of two ways: plasma processes operating in the shock front can produce a distribution which is a power law at each point (a 'local' power-law), or the superposition of non-power-law spectra (e.g. Maxwellians at different temperatures, possibly affected by radiative losses) can result in a 'global' power-law distribution. We concentrate mainly on local power-laws below. In the Appendix we show that the high frequency emission from an impulsive ER blast wave in which the electron distribution function is locally Maxwellian has a global spectral index of 4, larger than is observed.★

2.3 SYNCHROTRON SPECTRA

The synchrotron spectrum of an electron with the mean energy $\bar{\gamma}'_e m_e c^2$ reaches a maximum at a frequency

$$\bar{\nu}' = C\bar{\gamma}'^2_e B', \tag{10}$$

★ Examples of global power laws are provided by a NRAI blast wave in a uniform medium in which the pressure behind the shock is provided by relativistic electrons. The total relativistic electron distribution function predicted on the basis of the Sedov solution (e.g. Landau & Lifshitz 1959) is $dn/d\gamma'_e \propto \gamma'^{-7/3}_e$. This assumes that the particles are sufficiently strongly coupled to behave as a fluid. Alternatively if the electrons are able to move freely in the interior, but still suffer adiabatic decompression then $\gamma'_e \propto R^{-1}$ and $dn/d\gamma'_e \propto \gamma'^{-5/2}_e$. If the surrounding medium has a temperature $\gtrsim 10^{10}$ K, the shock will weaken and expansion cease whilst most of the electrons are relativistic and so a NRAI blast wave *could* be responsible for the acceleration and injection of relativistic electrons with energies $\lesssim 1$ GeV and approximately the correct distribution function into a compact radio source.

where $C = 1.0 \times 10^6$ Hz/G, for an isotropic distribution function. (We have used the rms perpendicular field component in deriving (10).) We express the post-shock magnetic field B' in terms of B_1 as

$$B' = 4k_B \Gamma B_1, \tag{11}$$

where k_B is of the order unity unless substantial field amplification occurs, as in galactic supernova remnants (Woltjer 1972). The corresponding frequency observed at Earth is $\bar{\nu} = k_\nu \Gamma \bar{\nu}'$ or

$$\bar{\nu} = 1.8 \times 10^{13} (k_e^2 k_\gamma^2 k_\nu k_B)\, \Gamma^4 \beta^4 B_1 \text{ Hz}, \tag{12}$$

measuring B_1 henceforth in gauss. This frequency lies above the radio band for ER blast waves unless the magnetic field is very small.

At sufficiently low frequencies, the source will be optically thick to synchrotron self-absorption and the flux S_ν will rise with frequency as ν^2 (Maxwellian) or $\nu^{2.5}$ (power law). The source becomes optically thin at sufficiently high frequencies, i.e. $S_\nu \propto \nu^{-\alpha}$ for $\nu < \nu_u$, with $\nu_u \sim \bar{\nu}$ and $\alpha = -\frac{1}{3}$ for a Maxwellian particle spectrum, whereas $\nu_u = k_\nu \Gamma C \gamma_u'^2 B'$ for a power law. The extrapolated optically thin and thick spectra intersect at the fiducial frequency ν_n where the flux would be S_n (Jones, O'Dell & Stein 1974, hereafter JOS).

When the source is optically thick, the flux from the source, which may be expanding relativistically, can be obtained by using the approximate Lorentz invariance of S_ν/ν

$$S_\nu = k_{\text{thk}}\, 2 \left(\frac{\gamma'_{\text{eff}} m_e c^2}{3}\right) \left(\frac{\nu'}{c}\right)^2 \left(\frac{\nu}{\nu'}\right) \frac{\pi R^2}{D^2}; \quad \nu < \nu_n \tag{13}$$

where k_{thk} is evaluated exactly for ER blast waves in the Appendix. In equation (13), $\gamma'_{\text{eff}} \equiv \bar{\gamma}'_e$ for a Maxwellian. For a power law, $\gamma'_{\text{eff}} \equiv (\nu'/CB')^{1/2}$ and

$$S_\nu = \frac{\pi}{3} \frac{m_e c^2}{C^{1/2} D^2} \left(\frac{k_{\text{thk}} k_o^2}{k_\nu^{3/2} k_B^{1/2}}\right) \Gamma^2 \beta^2 t_o^2 B_1^{-1/2} \nu^{5/2} \quad (\nu < \nu_n). \tag{14}$$

The optically thin flux can be obtained simply if one assumes that most of the observed emission lies in the optically thin part of the spectrum. For simplicity we shall assume that the emitted energy is concentrated at high frequencies ($\alpha < 1$), although our final result is more general. Under these assumptions the flux is related to the total synchrotron luminosity L_{so} observed at the redshift of the source by

$$S_\nu = \frac{k_{\text{thn}} L_{\text{so}}}{4\pi D^2} \left(\frac{\nu}{\nu_u}\right)^{-\alpha} \frac{(1-\alpha)}{\nu_u}; \quad \nu_n < \nu < \nu_u,\ \alpha < 1. \tag{15}$$

This result applies to a Maxwellian also if one sets $\alpha = -\frac{1}{3}$ and $\nu_u = \bar{\nu}$; k_{thn} is also discussed in the Appendix. The observed luminosity L_o is related to the emitted luminosity L' (in fact the sum of the emitted powers of the radiating particles which is Lorentz invariant), by

$$L_o = k_L \Gamma^2 L'. \tag{16}$$

If most of the emission occurs in the optically thin part of the spectrum, as we are assuming, then the emitted synchrotron luminosity is

$$L'_s = k_P \frac{4\pi}{3} R^3 n_1 \frac{4}{3} \sigma_T c \bar{\gamma}_e'^2 f u'_B, \tag{17}$$

where n_1 is the number density of electrons ahead of the shock, σ_T is the Thomson cross-

section, $u'_B = B'^2/8\pi$, and $f = \langle\gamma'^2_e\rangle/\bar{\gamma}'^2_e$ is proportional to the mean square electron energy, $\langle\gamma'^2_e\rangle$ of the emitting electrons. Inserting the appropriate expressions for $\bar{\gamma}'_e$ and B'^2, L_{so} can be expressed as

$$L_{so} = \frac{32}{9}\left(\frac{m}{m_e}\right)^2 \sigma_T\, c^4\, (k_L\, k_P k_o^3 k_e^2 k_\gamma^2 k_B^2)\, f\Gamma^2\beta^7 n_1 B_1^2 t_o^3, \tag{18}$$

so that

$$S_\nu = \frac{7.0\times10^{46}\,|1-\alpha|}{(1.8\times10^{13})^{1-\alpha}}\left(\frac{k_L\, k_P k_o^3 k_e^{2\alpha} k_\gamma^{2\alpha} k_B^{1+\alpha}}{k_\nu^{1-\alpha}}\right)\frac{g\,\Gamma^{8+4\alpha}\beta^{3+4\alpha} n_1 B_1^{1+\alpha} t_o^3}{D^2\nu^\alpha}\ \text{Jy} \tag{19}$$

where $g = k_{thn} f(\bar{\gamma}'_e/\gamma'_u)^{2(1-\alpha)}$ and n_1, t_o, D and ν are measured in cgs units. f and g are evaluated in the Appendix for adiabatic and radiative blast waves satisfying our assumption that most of the emission is in the optically thin part of the spectrum (i.e. $\alpha < 1$). If this assumption is not valid, then g must be redefined.

The time variations of the optically thin and optically thick synchrotron fluxes and other spectral quantities are tabulated in Table 2 for both non-relativistic and extreme relativistic

Table 2. Time variation of observable quantities for adiabatic blast waves.

X		$d\ln X/d\ln t_o$	
		NR	ER
$S_\nu(\nu<\nu_n)$	M	$\frac{4}{k_R}-2$	$\frac{2}{m+1}$
	PL	$\frac{8+k}{4k_R}$	$\frac{8+k+4m}{4(m+1)}$
$S_\nu(\nu>\nu_n)$		$-4\alpha+\frac{6-3k+\alpha(8-k)}{2k_R}$	$\frac{6-2m-3k-\alpha(4m+k)}{2(m+1)}$
S_n	M	$2+\frac{6-8k}{5k_R}$	$\frac{2(8-m-4k)}{5(m+1)}$
	PL	$\frac{1}{(5+2\alpha)}\left[-20\alpha+\frac{30-15k+4\alpha(12-k)}{2k_R}\right]$	$\frac{30-10m-15k+4\alpha(2-k-4m)}{2(m+1)(5+2\alpha)}$
ν_n	M	$2-\frac{(4k+7)}{5k_R}$	$\frac{3-m-4k}{5(m+1)}$
	PL	$\frac{2}{(5+2\alpha)}\left[-4\alpha+\frac{4-7k+2\alpha(8-k)}{4k_R}\right]$	$\frac{4-8m-7k-2\alpha(4m+k)}{2(m+1)(5+2\alpha)}$
$\bar{\nu}$		$-4+\frac{8-k}{2k_R}$	$-\frac{(4m+k)}{2(m+1)}$
L_{so}		$-4+\frac{7-2k}{k_R}$	$3-\frac{6m+2k}{m-1}$
$\frac{U'_S}{U'_B}=\frac{3b\phi_s}{b_{crit}}$		$-4+\frac{5-k}{k_R}$	$1-\frac{2m+k}{m+1}$
L_{co}		$-8+\frac{3(4-k)}{k_R}$	$4-\frac{(8m+3k)}{m+1}$
S_{cv}	PL	$-8\alpha+\frac{8-5k+\alpha(16-k)}{2k_R}$	$4-\left[\frac{10m+5k+\alpha(6m+k)}{2(m+1)}\right]$
ν_b		$-2+8i-\left[\frac{20i-k(3+4i)}{2k_R}\right]$	$\frac{4(im-i-i)+(3+4i)k}{2(m+1)}$

expansions, and for both Maxwellian and power-law distribution functions. Most of the results are valid only for the adiabatic case. We have assumed that $B_1^2 \propto n_1$ (so that the parameter b = const. in equation (4)), which is probably valid for both the uniform density and wind ($n_1 \propto R^{-2}$, $B_1 \propto R^{-1}$) cases, and also that the form of the particle spectrum is constant, so that g and α are constant. Explicit values for the time variations are given in Table 3, where we have used the values for m and k_R in Table 1. For comparison, the results for the standard, uniform expansion model (van der Laan 1966) are also given. The NRAI blast wave in a wind is probably closest to the standard model, since it has $\bar{\gamma}_e' \propto R^{-1}$, $B_1 \propto R^{-1}$, $n_1 \propto R^{-2}$ and $R \propto t^{2/3}$ instead of $\bar{\gamma}_e' \propto R^{-1}$, $B_1 \propto R^{-2}$, $n_1 \propto R^{-2}$ and $R \propto t$ for the standard model. An important difference between the blast wave and uniform expansion models is that the latter generally has more rapid time variations; for example, the optically thick flux $S_\nu \propto t_o^{5/3}$ for an NRAI shock in a wind whereas $S_\nu \propto t_o^3$ for the uniform expansion model. Hence, in fitting observed time variations, the blast wave model will give somewhat lower values for the age of a given outburst. In addition, estimates of the angular radius, θ, based on measurements of $d \ln S_\nu / d \ln t_o$ (Rees & Simon 1968) can be twice as large in the uniform expansion model as in the blast wave model.

Table 3. Spectral variation for adiabatic blast waves.

Energy supply	External medium	Distribution function	Shock velocity	$d \ln S_\nu / d \ln t_o$		$d \ln S_n / d \ln t_o$	$d \ln \nu_n / d \ln t_o$
				$\nu < \nu_n$	$\nu_u > \nu > \nu_n$		
Impulsive	Uniform	M	NR	−2/5	2	62/25	36/25
			ER	1/2	1/2	1/2	0
		PL	NR	4/5	$6(1-2\alpha)/5$	$(30-52\alpha)/5(5+2\alpha)$	$-4(6\alpha-1)/5(5+2\alpha)$
			ER	5/4	$-3\alpha/2$	$-5\alpha/(5+2\alpha)$	$-(6\alpha+5)/2(5+2\alpha)$
	Wind	M	NR	2/3	2/3	2/3	0
			ER	1	0	−1/5	−3/5
		PL	NR	5/3	-2α	$-20\alpha/3(5+2\alpha)$	$-2(5+6\alpha)/3(5+2\alpha)$
			ER	7/4	$-(3\alpha+1)/2$	$-(8\alpha+5)/2(5+2\alpha)$	$-3(2\alpha+3)/2(5+2\alpha)$
Steady injection	Uniform	M	NR	2/5	7/3	68/25	29/25
			ER	1	4/3	7/5	1/5
		PL	*NR*	*6/5*	$(9-8\alpha)/5$	$(45-28\alpha)/5(5+2\alpha)$	$2(3-8\alpha)/5(5+2\alpha)$
			ER	*3/2*	$1-\alpha$	$(5-2\alpha)/(5+2\alpha)$	$-(2\alpha+1)/(5+2\alpha)$
	Wind	M	NR	2	1/3	0	−1
			ER	2	1/3	0	−1
		PL	NR	5/2	$-\alpha$	0	−1
			ER	5/2	$-\alpha$	0	−1
Standard model★		PL	NR	3	$-2(2\alpha+1)$	$-2(5+7\alpha)/(5+2\alpha)$	$-2(5+4\alpha)/(5+2\alpha)$

★ e.g. van der Laan 1966.

A real source may not confine itself to one of the cases in Table 3. The expansion could evolve from ER to NR or from radiative to adiabatic; it could begin with a phase of steady injection and then develop into an impulsive blast wave if the power supply is turned off; or it could start in a wind and then expand into a region of almost uniform density where the momentum flux in the wind balances the ambient external pressure.

2.4 INVERSE COMPTON RADIATION AND THE RADIATIVE EFFICIENCY

In addition to emitting synchrotron radiation, the relativistic electrons accelerated by the shock can Compton scatter the synchrotron photons to higher energies. This has long constituted both a feature and a constraint of existing models of variations in galactic nuclei (Hoyle, Burbidge & Sargent 1966; Rees 1967b; JOS).

The inverse Compton emissivity in the comoving frame is proportional to the energy density of radiation in that frame. The synchrotron radiation energy density u'_s can be related to the emitted luminosity L'_s (equation (17)) by

$$u'_s = \frac{k_u k_L L'_s}{2\pi R^2 c} \tag{20}$$

The factor k_L from equation (16) has been inserted because it includes the effect of radiation emitted at earlier times. The emitted luminosities of once- and twice-scattered inverse Compton radiation are given by

$$L'_c = \left(\frac{u'_s}{u'_B}\right) L'_s, \tag{21}$$

$$L'_{cc} = \left(\frac{u'_s}{u'_B}\right)^2 L'_s \tag{22}$$

in obvious notation. Further Compton scatterings are suppressed when the Klein–Nishina cross-section becomes appropriate (Rees 1967b), and in fact L'_{cc} may be suppressed below the value given in equation (22) if the synchrotron luminosity is primarily at high (e.g. optical) frequencies. The ratio u'_s/u'_B can be written

$$\frac{u'_s}{u'_B} = \left(\frac{k_u k_L}{k_B^2 k_o^2}\right) \frac{6L'_s}{32\pi\rho_1 c^5 \Gamma^6 \beta^2 t_o^2} \tag{23}$$

by using equation (11) for B' and equation (4) for B_I^2.

We next define a radiative efficiency, ϕ, as being the ratio of the instantaneous emitted power L' to the power supplied to the electrons. For steady injection, we approximate the power supplied to the electrons, $k_e(1-\beta_s)L_I$ by $k_e L_I/\Gamma^2$, where β_s is the velocity of the shock in the injection fluid (see Paper I). In this case $\phi = \Gamma^2 L'/k_e L_I = L_o/k_e k_L L_I$. For an adiabatic impulsive blast wave, we use $k_e E/t$ for the power supplied. Then, using equations (1) and (2), we find that in both cases

$$\phi = 3L'/[(k_R k_o^2 k_\sigma k_u k_e)\, 4\pi\rho_1 c^5 \Gamma^6 \beta^5 t_o^2]\,. \tag{24}$$

The ratio u'_s/u'_B can be expressed in terms of the synchrotron efficiency $\phi_s \propto L_s$ as

$$\frac{u'_s}{u'_B} = \frac{3b\phi_s}{b_{crit}} \tag{25}$$

where

$$b_{crit} = 72\,[(k_B^2)/(k_R k_L k_u k_\sigma k_e k_w)]\,\beta^{-3}. \tag{26}$$

Then the once- and twice-scattered Compton efficiencies become

$$\phi_c = (3b/b_{crit})\,\phi_s^2, \tag{27}$$

$$\phi_{cc} = (3b/b_{crit})^2\,\phi_s^3. \tag{28}$$

A *radiative* shock is then one for which $\phi \sim 1$. Since $\phi = \phi_s + \phi_c + \phi_{cc}$, we see that for such a shock $b = b_{crit}$ implies $\phi_s = \phi_c = \phi_{cc} = 1/3$. For smaller values of b, a radiative shock is synchrotron dominated, whereas for larger values it is Compton dominated. (If the twice-scattered luminosity is suppressed, the break between Compton and synchrotron dominated shocks occurs at $b = 2/3 b_{crit}$.) Note that $b \sim b_{crit}$ does not ensure that the shock is radiative, and that an ER shock with $b \ll b_{crit}$ violates our assumption that the magnetic field is not dynamically important (equation (5)).

For any shock the relation between the total radiative efficiency ϕ and the synchrotron efficiency ϕ_s is approximately

$$\phi = k_\phi \phi_s (3b\phi_s/b_{crit})^i \tag{29}$$

where $i = 0$ if the radiation is primarily synchrotron emission ($3b\phi_s/b_{crit} < 1$), and $i = 1$ or 2 if once- or twice-scattered Compton radiation dominates the luminosity ($3b\phi_s/b_{crit} > 1$).

For a power-law electron distribution, the Compton-scattered synchrotron spectrum extends from $\sim \gamma_1^2 \nu_n$ to $\sim \gamma_u^2 \nu_u$, assuming that the low-frequency turnover is due to synchrotron self-absorption and the Klein–Nishina cut-off does not apply. For $\alpha < 1$ the spectrum of the scattered radiation is about $S_{cc\nu}/S_{c\nu} \sim S_{c\nu}/S_{s\nu} \sim (\gamma_u')^{-2(1-\alpha)} (u_s'/u_B')$, where $S_{s\nu}$ is the synchrotron flux, $S_{c\nu}$ the once-scattered Compton flux at the same frequency etc. A more precise value can be obtained by adapting the quantity, $E_\nu^{sc} = S_{c\nu}/S_{s\nu}$ derived in JOS, to the blast-wave model

$$\frac{S_{c\nu}}{S_{s\nu}} = \frac{1.5 \times 10^{-40}}{(1.1 \times 10^7)^{1+\alpha}} \left(\frac{k_u k_\nu^{1-\alpha} e_{\alpha 0}^{sc} \ln \Lambda}{k_B^{1+\alpha} k_o^2} \right) \frac{D^2 S_{s\nu} \nu^\alpha}{B_1^{1+\alpha} \Gamma^{6+2\alpha} \beta^2 t_o^2} \text{ Jy}, \tag{30}$$

where $e_{\alpha 0}^{sc}$ is tabulated as a function of α in JOS and $\ln \Lambda$ is typically $\ln(\nu_u/\nu_n)$. These spectra are displayed schematically in Fig. 1.

Finally, as discussed further in Section 5, we note that if the energy in the steady injection case is supplied by ultrarelativistic particles, then these may be subject to inverse

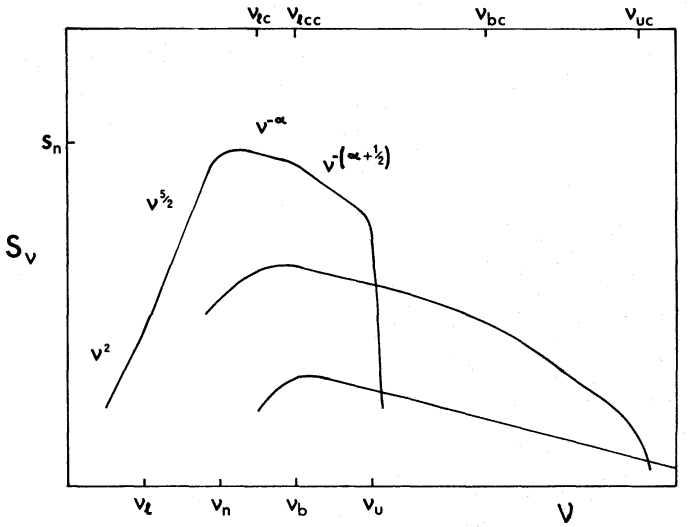

Figure 1. Schematic Compton–Synchrotron spectrum from an expanding blast wave. The electron distribution function is assumed to be $dn/d\gamma_e' \propto \gamma_e'^{-s_i}$, $\gamma_1 \lesssim \gamma_e' \lesssim \gamma_b'$ and $dn/d\gamma_e' \propto \gamma_e'^{-(s_i+1)}$, $\gamma_b' \lesssim \gamma_e' \lesssim \gamma_u'$ where s_i is the energy exponent of the injected electrons and radiative losses account for the steepening at high energies. The observed synchrotron spectrum becomes optically thin at ν_n (greater than ν_e, the characteristic frequency of electrons with energy γ_e' in this example) and extends up to ν_u through ν_b where the spectral index α increases by ½. The Compton spectrum extends from $\nu_{1c} \sim \gamma_e^2 \nu_n$ to $\nu_{uc} \sim \gamma_u^2 \nu_u$, breaking at $\nu_{bc} \sim \gamma_b^2 \nu_b$. Twice-Compton-scattered photons have frequencies $\nu \gtrsim \nu_{1cc} \sim \gamma_1^4 \nu_n$.

Compton losses also. The electron distribution in the shocked injection fluid probably extends to much higher energies than in the shocked external medium, and the energies of the scattered photons will be correspondingly higher.

2.5 RADIATIVE LOSSES

Synchrotron and inverse Compton losses vary as the square of the electron energy and therefore tend to steepen the high-energy portion of the electron distribution. A measure of the energy at which radiative losses are important is the energy γ'_b at which the loss time equals the expansion time. Electrons with $\gamma'_e > \gamma'_b$ will have a shorter loss time and thus their distribution will be approximately in a steady state in which the steady injection by the shock (at a rate $Q(\gamma'_e)$ is balanced by the radiative losses (at a rate $\dot{\gamma}'_e$). The electron distribution is then given by (e.g. Pacholczyk 1970)

$$\frac{dn}{d\gamma'_e} = \frac{1}{\dot{\gamma}'_e}\int_{\gamma'_e}^{\infty} Q(\gamma''_e)\, d\gamma''_e. \tag{31}$$

For an injection spectrum $Q(\gamma'_e) \propto \gamma'^{-s_i}_e$, we find $s = s_i + 1$ if $s_i \geqslant 1$; however, if $s_i < 1$ (as for a Maxwellian at $\gamma'_e \lesssim K_B T/m_e c^2$) then $s = 2$. Hence a steady state, loss-dominated distribution cannot be flatter than $s = 2$, corresponding to $\alpha = \frac{1}{2}$. We shall now evaluate the energy, γ'_b at which radiative losses are important; the result will be valid for both radiative and adiabatic shocks. Then we shall determine the condition for a blast wave to be radiative.

The defining condition for γ'_b is

$$\frac{\gamma'_b m_e c^2}{t/\Gamma} = \tfrac{4}{3}\sigma_T c \left(\frac{k_P k_\gamma}{k_\sigma k_w}\right) \gamma'^2_b\, (u'_B + u'_s + u'_c), \tag{32}$$

where we have taken the expansion time to be t/Γ and where the once-scattered Compton energy density u'_c should be omitted if the second scattering is suppressed. The factor $(k_P k_\gamma / k_\sigma k_w)$ has been inserted in order to simplify equation (36) below. The sum of the energy densities in equation (32) is simply $u'_B(\phi/\phi_s)$ so that

$$\frac{\gamma'_b}{\gamma'_e} = \frac{3\pi}{8}\frac{m_e^2 c}{\sigma_T m}\left(\frac{k_\sigma k_R k_w}{k_B^2 k_e k_\gamma^2 k_o k_P}\right)\frac{\phi_s}{\phi}\frac{1}{\Gamma^4 \beta^2 B_1^2 t_o} \tag{33}$$

The corresponding synchrotron frequency is $\nu_b = (\gamma'_b/\bar{\gamma}'_e)^2 \bar{\nu}$, where $\bar{\nu}$ is given in equation (12)

$$\nu_b = 9.3 \times 10^{21}\left(\frac{k_\sigma^2 k_R^2 k_\nu k_w^2}{k_P^2 k_B^3 k_\gamma^2 k_o^2 k_\phi^2}\right)\left(\frac{3b\phi_s}{b_{\rm crit}}\right)^{-2i}\frac{1}{\Gamma^4 B_1^3 t_o^2}\ \text{Hz}. \tag{34}$$

Here we have used equation (29) for ϕ_s/ϕ. Note that an upper bound on ν_b is obtained by setting $i = 0$ (i.e. assuming the blast wave is synchrotron dominated), since $i \geqslant 1$ implies $(3b\phi_s/b_{\rm crit}) > 1$.

If $\gamma'_b/\bar{\gamma}'_e \lesssim 1$, the shock is radiative since most of the electron energy is radiated away and $\phi \sim 1$. This is not a necessary condition for a radiative shock, however, since if the electron distribution is a power law with $2 > s > 1$ most of the energy can be concentrated in electrons with $\gamma'_e \gg \bar{\gamma}'_e$; in this case a radiative shock can occur even if $\gamma'_b \gg \bar{\gamma}'_e$. To obtain a general necessary condition for a shock to be radiative, we shall first assume that it is adiabatic and then determine the value of L_{so} at which $\phi = 1$.

Inserting expression (17) for L'_s into equation (24) gives

$$\phi_s = \frac{8}{3\pi}\frac{m\sigma_T}{m_e^2 c}\left(\frac{k_\gamma^2 k_B^2 k_P k_o k_e}{k_R k_\sigma k_w}\right)\Gamma^4\beta^2 f B_1^2 t_o, \tag{35}$$

where it is assumed that most of the emission is in the optically thin part of the spectrum. We then obtain the simple result

$$\gamma'_b/\bar{\gamma}'_e = f/\phi, \tag{36}$$

where the quantity f is given as a function of γ'_u and $\bar{\gamma}'_e$ in the Appendix. In particular, for a flat injected distribution ($1 < s_i < 2$) with $\gamma'_b \ll \gamma'_u$, we find $f = \gamma'_b/\bar{\gamma}'_e$ and $\phi = 1$; this was to be expected, since most of the energy in a flat distribution is concentrated near γ'_u. Using equation (24) to obtain $B_1^2 \propto \rho_1/b$ in terms of L'_s and ϕ_s and inserting the result into equation (35) yields

$$L_{so} = \frac{3\pi}{2}\frac{m_e^2 c^4}{m\sigma_T}\left(\frac{k_R k_o k_\sigma k_w}{k_\gamma^2 k_P k_u k_e}\right)\left(\frac{3b}{b_{crit}}\right)\frac{\phi_s^2\Gamma^4 t_o}{f}. \tag{37}$$

With the aid of equation (29) we finally obtain

$$L_{so} = 2.4\times 10^{36}\left(\frac{k_R k_o k_\sigma k_w}{k_\gamma^2 k_P k_u k_e}\right)\left(\frac{\phi}{k_\phi}\right)^{2/(1+i)}\left(\frac{3b}{b_{crit}}\right)^{(1-i)/(1+i)}\frac{\Gamma^4 t_o}{f}\ \text{erg/s}. \tag{38}$$

Since $\phi < 1$ and $f > 1$ for an adiabatic shock, a sufficient condition for a radiative shock is that the observed synchrotron luminosity exceed the value in equation (38) with $\phi = 1$, $f = 1$, $k_\phi = 1$ and $i = 1$; this is equivalent to requiring that $\gamma'_b < \bar{\gamma}'_e$.

3 Variable radio sources

3.1 GENERAL FEATURES

As mentioned in the Introduction, the simple uniform expansion model of compact variable radio sources encounters several problems when confronted with some more recent data (e.g. Medd *et al.* 1972; Altschuler & Wardle 1976). The nature of these difficulties is discussed by BJO and references therein. In many sources (e.g. Locke, Andrew & Medd 1969) the variation of the flux density with frequency and time shows *qualitative* disagreement with the simple model in that, for example, the high-frequency flux does not peak before that at low frequency, the rate of decrease of flux is very much faster than the rate of increase and the low-frequency spectral index significantly exceeds -2.5. Various modifications (e.g. Hirasawa & Tabara 1970; Peterson & Dent 1973; Condon & Dressel 1973; de Bruyn 1976) have been proposed involving continuous injection and spatial inhomogeneity to account for these discrepancies. Furthermore, *VLB* studies of some of these sources have shown them often to be resolved into separating doubles. The phenomenological model of Ozernoi & Sazonov (1969) can account for this feature. Although we do not pursue the matter much further here, modifications of the simple geometrical and, in particular, particle acceleration hypotheses made in the previous section should be able to account for most of the spectral and morphological variations observed. Even the very restrictive set of assumptions used in Table 3 leads to a wide variety of spectral forms.

Of more fundamental importance are the *quantitative* objections that have been raised against the synchrotron interpretation of radio variability. In this section we demonstrate that relativistic blast-wave models can generally overcome the most serious objections to

the uniform expansion model without invoking completely unrealistic quantities of unobserved energy. (The objection raised by BJO against relativistically expanding models – that the increased source volume and the large additional amount of non-useful work done pushing against the surrounding medium lead to an unacceptable average power requirement – does not apply in the present context).

Most, but not all, of the well-studied outbursts show a high-frequency flux density that decays as a power of time and a spectral index $\alpha \sim 0.25$ (e.g. Dent 1968). From Table 3 we see that this behaviour cannot be reproduced by a Maxwellian distribution function, and so we confine our attention to power-law distributions.

We assume that $S_\nu(\nu, t_o)$ is known for the outburst, choosing the time origin either by extrapolation or possibly by means of an earlier outburst at much higher frequency (*cf.* Usher 1972). We also assume that an adequate estimate of θ can be obtained from *VLB* observations and that β can be inferred either by understanding the kinematics or by using equation (7), (8).

From the flux S_n and frequency ν_n of the turnover in the radio spectrum (assumed to be due to synchrotron self-absorption), we can solve equation (14) to obtain

$$B_1 = \left(\frac{\pi m_e}{3C^{1/2}}\right)^2 \frac{k_{thk}^2 \theta^4 \nu_n^5}{k_\nu^3 k_B k_\theta^4 S_n^2} \tag{39}$$

In the NR limit, the shocked field strength, $B' = 4B_1$, agrees with the usual result (e.g. JOS) The ambient density, n_1, can then be inferred from equation (19) provided that enough is known about the spectrum to estimate g and that $\nu_b > \nu_n$. Next the total explosion energy (or power in the SI case) can be calculated from equation (1) or (2).

The inverse Compton luminosity is determined by the ratio u_s'/u_B' (equation (23)), which can be expressed in terms of the characteristic synchrotron frequency $\bar{\nu}$ (equation (12)) as

$$\frac{u_s'}{u_B} = \frac{3b\phi_s}{b_{crit}} = 3.1 \times 10^6 \left(\frac{k_u k_\nu^2 k_e^4 k_\gamma^4}{k_o^2}\right) \frac{\beta^6 L_{so\,42}}{\bar{\nu}_9^2 t_{o6}^2}, \tag{40}$$

where $L_{so\,42} = L_{so}/(10^{42}\,\mathrm{erg/s})$, $t_{o6} = t_o/(10^6\,\mathrm{s})$, etc. An equivalent relation in terms of the peak brightness temperature, $T_n = 10^{12} T_{n\,12}\,\mathrm{K}$, as measured by *VLBI* is

$$\frac{u_s'}{u_B'} = 0.10 \frac{k_u k_\theta^{10} k_\nu^6}{(1-\alpha)\, k_{thn} k_{thk}^4} \frac{T_{n\,12}^5 \nu_{n9}^\alpha \nu_{u9}^{1-\alpha}}{\Gamma^6}, \quad \alpha < 1. \tag{41}$$

This generalizes the well-known non-relativistic expression due originally to Kellermann & Pauliny-Toth (1969).

A useful restriction can be placed on L_{so} if there is an upper bound on $\bar{\nu}$. Such a bound exists if the spectrum below ν_b is steep, i.e. $\alpha_i = \frac{1}{2}(s_i - 1) > \frac{1}{2}$ (see Section 2.5), then $\bar{\nu} \sim \nu_1$ and, in the optically thin part of the spectrum, $\nu > \nu_n \gtrsim \bar{\nu}$. An observational bound on the once-scattered Compton luminosity L_c can be obtained directly from optical and X-ray observations and indirectly from an analysis of the emission lines excited by UV radiation. Altogether we find

$$L_{so\,42} \lesssim 0.056 \left(\frac{k_{\bar{o}}}{k_u^{1/2} k_\nu k_e^2 k_\gamma^2}\right) \frac{\nu_{n9} t_{o6} L_{c\,46}^{1/2}}{\beta^3} \tag{42}$$

for $\alpha_i > \frac{1}{2}$. In particular, if the observed spectral index α exceeds 1, then $\alpha_i > \frac{1}{2}$ and this inequality holds. For $1 > \alpha > \frac{1}{2}$, violation of this inequality would indicate $\nu_b < \nu$ and that the shock is radiative ($\phi \sim 1$). ϕ_s can then be calculated from equation (29). Alternatively,

if β is known sufficiently accurately we can use the value of $\bar{\nu}$ calculated from the field, equation (39), to obtain a theoretical limit on the synchrotron power.

A practical difficulty arises in applying equation (40) to estimate ϕ_s: for $\alpha < 1$, most of the luminosity lies in the inaccessible far-infrared part of the spectrum so that L_{so} is not known. If $\frac{1}{2} < \alpha_i < 1$, the spectrum can be cut off at ν_b as given by equation (34) to provide an upper limit on L_{so}. However, for flatter spectra, $-\frac{1}{3} < \alpha_i < \frac{1}{2}$, only a lower limit can be obtained by using the highest frequency at which the outburst is observed.

3.2 3C120

The Seyfert galaxy 3C120 is perhaps the most intensively studied extragalactic radio source (e.g. Pauliny-Toth & Kellermann 1968). Seielstad (1974) has summarized the available data from mid-1967 to the end of 1973 which he fits to five successive outbursts of the type discussed by Ozernoi & Sazonov (1969). A relatively 'clean' outburst for which *VLB* observations are available reached maximum in 1972 October when $\theta \sim 0.3$ milliarcsec (Kellermann *et al.* 1973), $S_n = 8$ Jy, $\nu_n = 10$ GHz. (Following BJO we associate half the measured flux with 2θ, the half-power beamwidth.) It is difficult to estimate the age t_o because of confusion with an earlier outburst. As it is ~ 1 yr, we have calculated two spherical models, I and II, corresponding to expansion velocities, $\Gamma\beta = 0.5, 1$, i.e. $t_o = 3.7 \times 10^7$s, 2.8×10^7s respectively. These models still have too many free parameters to be specified uniquely unless we make some additional assumptions about the spectrum. Following Seielstad we choose $\alpha_i = 0.25$. The qualitative spectral variation seems most compatible with an explosion in a non-relativistic wind ($k_w = 1, k = 2$) although the data are strictly inadequate to exclude any of the other possibilities in Table 3. For model I we have assumed that the explosion is adiabatic-impulsive and have further constrained the solution by assuming that the upper cut-off ν_u equals the break frequency ν_b defined by equation (34). Model II is radiative however, and so we use the k factors appropriate to a steady injection explosion. In this latter model the equations are supplemented by the arbitrary assumption $b = b_{mag}$. In both models we assume equipartition between the ions and the electrons behind the shock, i.e. $k_e = 0.5$. As the expansion speed is mildly relativistic, most of the constants k_x must be interpolated between the NR and ER values. We use the formula

$$k_x = k_x(\mathrm{NR})^{[\frac{1}{2} - \log_{10}(\Gamma\beta)]}\, k_x(\mathrm{ER})^{[\frac{1}{2} + \log_{10}(\Gamma\beta)]}; \quad 10^{-1/2} \leqslant \Gamma\beta \leqslant 10^{1/2}. \tag{43}$$

We can now calculate uniquely the remaining parameters for the two models, fitting the peak value of the flux in 1972 October. The results are displayed in Table 4. Model I is fairly radiative ($\phi = 0.33$) and synchrotron dominated and so the total energy requirements do not greatly exceed the integrated radio power. There is no need to invoke large quantities of invisible energy in a shock wave model (*cf.* BJO). The predicted (Compton scattered) optical flux is insignificant. Model II by contrast is Compton dominated and the synchrotron spectrum extends up to $\sim 2 \times 10^{15}$ Hz. It therefore requires ~ 1000 times more energy than the integrated radio power. However, the predicted optical flux at 10^{15} Hz is ~ 2 mJy, comparable with that actually observed by Kinman (1968) and so this model could explain correlated optical and radio variability. As the optical emission is synchrotron radiation, it need not have such a rapid evolution with time as the inverse Compton model of Peterson & King (1975). There are two types of observations that could restrict the class of acceptable models; more accurate mm observations, in particular the resolution of spectral breaks attributable to radiative cooling, and firmer evidence for correlated radio and optical variation.

3.3 LOW-FREQUENCY VARIABILITY

Hunstead (1972) and Cotton (1976) have presented evidence that in a small minority of compact sources there is significant variability at low radio frequencies, where the spectrum

Table 4. Models for 3C120.

Model	I (AI)	II (SI)	Model	I (AI)	II (SI)
$\Gamma\beta$	0.5	1.0	$t_o(10^7\,s)$	3.7	2.8
Γ	1.12	1.41	$R(10^{18}\,cm)$	1.1	1.6
β	0.45	0.71	γ'_e	92	365
k_θ	0.91	0.76	B_1 (G)	0.036	0.033
k_o	1.76	1.37	ν (GHz)	1.4	33
k_R	1.38	1.0	ν_b (GHz)	200★	24
k_{thk}	0.64	0.47	ν_u (GHz)	200★	1.8×10^6
k_{thn}	0.73	0.73	$n_1(cm^{-3})$	6.5	1.7
k_B	0.93	0.34	b	220	70★
k_ν	1.04	1.15	b_{mag}	230	70★
k_σ	1.38	6.36	b_{crit}	140	8.9
k_L	1.70	1.41	ϕ_s	0.15	0.10
k_P	0.96	2.51	ϕ	0.33	1.0
k_γ	0.38	0.48	$L_{so}(10^{44}\,erg/s)$	0.63	6.5
k_e	0.5	0.5	L_{co} $(10^{44}\,erg/s)$	0.44	16.2
k_u	3	3	S_ν(mJy; 10^{15} Hz)	0.018†	2.2†
k_w	1	1	$E/L_1 t(10^{52}\,erg)$	21	71

★ Assumed to be the same.
† Inverse Compton radiation in I, synchrotron radiation in II.

appears to be optically thin. These sources are characterized by variability timescales at least an order of magnitude smaller than the inferred source sizes in units of c. If they are to be interpreted as blast waves then ER motion is clearly indicated.

The evidence for low-frequency flux variations is still controversial and as yet there are no corresponding low-frequency *VLB* variability studies. However, as an example of the application of our calculations, we follow BJO and consider CTA102. We adopt a flux of 3.5 Jy at 460 MHz, with a measured angular radius of 3.5 milliarcsec varying on a timescale of 2.3 yr. Because the spectrum is fairly flat, $\nu_n \sim 460$ MHz, which implies that $B_1 \sim 6 \times 10^{-4}$G, (equation (39)). If $t_o \sim 2.3$ yr, then $\Gamma \sim 40$ and the source radius is ~ 4 kpc, at least two orders of magnitude larger than normally contemplated in these sources. If $\alpha > 0.5$, then $\nu \sim \bar{\nu}$, $B_1 \sim 10^{-10}$G and the shock is strongly Compton-dominated, with prohibitive power requirements. Even if we increase $\bar{\nu}$ to $\sim 3 \times 10^{11}$ Hz, which is the maximum value it can have and be consistent with radio and optical observations, the magnetic field strength is still too low for a viable model.

The nature of the difficulty is made apparent by rewriting equations (17), (24) in the form

$$\phi_s = 1.5 \times 10^{-7} \left(\frac{k_P k_o}{k_e^3 k_\sigma k_w k_R k_\gamma^2 k_\nu^2} \frac{f \bar{\nu}_9^2 t_{o6}}{\Gamma^4 \beta^6} \right). \tag{44}$$

In order that most of the synchrotron power be concentrated at radio wavelengths, $\bar{\nu}_9 \lesssim 10$ and we see that an ER blast wave is necessarily very inefficient. (For CTA102, $\phi_s \sim 10^{-7}$.)

There is an alternative possibility however. If the external medium is inhomogeneous on length scales comparable with the observed radio size, then variability can be seen on a timescale $\sim \Gamma^{-1} t_o$. In this case, the variation should have the appearance of fluctuations superimposed on a longer term trend. So, using a lower shock Lorentz factor $\Gamma \sim 6$, and an observed age $t_o \sim 15$ yr, we have calculated an adiabatic impulsive model consistent with observations. The radio spectrum extends up to $\nu_u \sim 3 \times 10^{13}$ Hz with a spectral index of 0.25 and the total synchrotron power (mainly in the infrared) is $L_{so} \sim 10^{46}$ erg/s. The shock

is marginally radiative with $\phi_s \sim \phi_c \sim 0.3$ so that there is a Compton-scattered γ-ray luminosity $\sim 10^{48}$ erg/s. The total energy requirement $\sim 3 \times 10^{57}$ erg. The present physical size of the source would have to be $R \sim 600$ pc and the density and field in the external medium would be $n_1 \sim 4 \times 10^{-6}\,\mathrm{cm}^{-3}$, $B_1 \sim 8 \times 10^{-5}$ G. These parameters differ substantially from their counterparts in the models of 3C 120.

4 Optical and X-ray outbursts

4.1 GENERAL FEATURES

The optical continua from many active galactic nuclei and quasars are observed to have power-law spectra, to be appreciably polarized (~ 10 per cent), and to vary on timescales which are typically of order weeks (e.g. O'Connell 1971; Visvanathan 1973). It is generally assumed that the emission is due to synchrotron radiation or inverse Compton scattering of radio-frequency synchrotron photons. (Models have also been constructed in which the emission is attributed to non-relativistic Compton scattering – Colgate, Colvin & Petschek 1975; Katz 1976 – but we do not consider these here.)

The central theoretical problem with these models is that the radiation losses are so severe that the radiative lifetime of an electron is much less than the light travel time across the source (Hoyle, Burbidge & Sargent 1966; Demoulin & Burbidge 1968). The short radiative lifetime of the electrons causes no problems in the blast-wave model because electrons are continuously accelerated in the shock. Synchrotron models can be very efficient, with most of the electron energy being converted to optical radiation, whereas in the conventional Compton models most of the energy appears as doubly scattered photons in the hard X-ray or γ-ray region of the spectrum.

If the optical radiation is due to synchrotron emission, it is a simple matter to show that the blast wave is radiative unless it is extremely relativistic. Equations (24), (29), and (33) give

$$\frac{\gamma_b'}{\bar{\gamma}_c'} = 2.4 \times 10^{-4} \left(\frac{k_\sigma k_R k_o k_w}{k_P k_e k_\gamma^2 k_u k_\phi} \right) \left(\frac{3 b \phi_s}{b_{\mathrm{crit}}} \right)^{1-i} \frac{\Gamma^4 t_{o6}}{L_{so46}} \tag{45}$$

for the Lorentz factor γ_b' at which radiative losses set in. Since $(3b\phi_s/b_{\mathrm{crit}})^{1-i} \leqslant 1$, we find that for a rapidly varying, luminous source ($t_{o6} \lesssim 1$, $L_{so46} \gtrsim 0.1$) we have $\gamma_b'/\bar{\gamma}_e' < 1$, unless $\Gamma \gg 1$, which is a sufficient condition for a radiative shock.

The inverse Compton problem occurs in quasar models only if the radiative lifetime of the electrons is constrained to be greater than the light travel time across the source. This is necessary in a blast wave model only if the spectrum is observed to be flat ($\alpha < \frac{1}{2}$), since as shown in Section 2.5) radiative losses steepen spectra to $\alpha > \frac{1}{2}$. So, if the optical spectrum is observed to be flat, then $\nu_b > \nu \sim 10^{15}$ Hz. Using this inequality together with equation (34) we find

$$t_{o6} \gtrsim 1.0 \times 10^{8} \left(\frac{k_\phi^{3/2} k_u^{3/2} k_P^2 k_\gamma^2}{k_w^2 k_R^2 k_o k_\nu k_\sigma^2} \right) \frac{L_{so46}^{3/2} \nu_{15}}{\Gamma^8 \beta^3}. \tag{46}$$

Hence, t_o is comparable with the observed timescales $\sim 10^{6-7}$ s only if $\Gamma \gtrsim 10$ or $L_{so} \ll L_{\mathrm{optical}}$. We conclude that luminous variable optical sources with flat spectra ($\alpha < \frac{1}{2}$) can be synchrotron emitters only if the expansion is extremely relativistic. If $\alpha > \frac{1}{2}$, then the blast wave must be radiative with $\nu_b < \nu$. Observationally, most optically variable quasars have steep spectra (Oke, Neugebauer & Becklin 1970), so there need be no difficulty with assuming the optical emission to be due to synchrotron radiation.

4.2 OPTICAL SYNCHROTRON RADIATION: AO 0235+164

An example of an optically variable object for which conventional theoretical interpretations are severely strained and for which good observational data are available is AO 0235+164. This is a BL Lac-type object, which has recently undergone a particularly violent outburst, described by MacLeod, Andrew & Harvey (1976), Ledden, Aller & Dent (1976) and Rieke *et al.* (1976). This outburst was unusual because the radio and optical fluxes varied simultaneously. As these authors remark, the radio brightness temperature inferred on the basis of an assumed source size $\lesssim c\,t_o$ is $T_B \gtrsim 10^{15}$ K. A viable blast-wave model must therefore be extremely relativistic (*cf.* equation (41)). The high-frequency radio spectral index is 0.15 and from Table 3 we see that the observed flux variation is most consistent with steady injection and a uniform external medium ($S_n \propto t_o^{0.89}$, $\nu_n \propto t_o^{-0.25}$, $S_n \propto \nu_n^{-3.6}$) although, as this assumes a constant value for g, the other possibilities cannot strictly be rejected.

Most of the observed power is in the near-infrared ($\sim 10\,\mu$m) and the spectrum is extremely curved so that the B spectral index ~ 4. This is attributable either to an intrinsic cut-off in the emitted spectrum or to subsequent reddening. The absence of any appreciable colour change during the outburst and the large value inferred for the gas column density along the line of sight (Rieke *et al.* 1976) both support the latter interpretation.

We make the simplest assumptions about the synchrotron spectrum; that it extends from a turnover frequency ν_n to a break frequency ν_b with a spectral index α_i and thence through the observed 10-μm value to an upper cut-off frequency ν_u with $\alpha = \alpha_i + 0.5$. (As the results are fairly sensitive to the adopted values of S_n, ν_n which are only determined to within a factor two by the radio observations, it is necessary to regard these quantities initially as free parameters.)

As long as $\alpha_i < 0.5$, the observed synchrotron luminosity is given by equation (15) as

$$L_{so\,48} = [4.3\,(0.030)^{\alpha_i}\,S_\nu\,(10\,\mu\text{m})\,\nu_{u15}^{0.5-\alpha_i}\,D_{28}^2]\,/k_{thn}\,(1-2\alpha_i) \tag{47}$$

measuring S_ν in Jy. The synchrotron spectrum extends up to so high a frequency that only one Compton scattering is possible. We can then combine equations (14), (19), (20), (24), (29), (47) to eliminate Γ, B_1, n_1 and L_{so} and obtain

$$\left(\frac{u_s'}{u_B'}\right)^{0.5} + \left(\frac{u_B'}{u_s'}\right)^{0.5} = \frac{0.034\,D_{28}\,k_{thn}^{0.5}\,(1-2\alpha_i)^{0.5}\,\phi S_n^2}{(520)^{\alpha_i}\,k_{thk}\,t_{o7}^2\,\nu_{n10}^{2.5-\alpha_i}\,S_\nu^{1.5}\,(10\,\mu\text{m})\,\nu_{u15}^{(0.25-0.5\alpha_i)}}. \tag{48}$$

In equation (48) the degree of synchrotron/Compton dominance is expressed in terms of observable quantities. In general there will be either both a synchrotron-dominated and a Compton-dominated solution or no solution at all for a given set of spectral assumptions. The most economical blast waves are those for which $u_s' = u_B'$ and we have calculated two such models incorporating the two different assumptions about the optical spectrum. In both models we assume $D_{28} = 2.3$ (corresponding to the larger measured redshift, $z = 0.85$), S_ν (10 μm) = 0.5 Jy, and $t_{o7} = 1$ which corresponds to the time the radio flux took to reach maximum. (The optical emission showed variability on shorter timescales, but this we attribute to inhomogeneity in the surrounding medium, to which relativistic, radiative shocks are especially sensitive.) In addition we adopt the ER values of k_x given in the appendix plus the assumptions: $k_e = 0.5$, $k_w = 1$, $k_u = 2$.

In the first model, the steep optical spectrum is assumed to be produced extrinsically (i.e. by reddening) and we choose $\nu_n = \nu_1 = 10$ GHz and $\alpha_i = 0.15$, the radio spectral index quoted by Ledden *et al.* (1976). The requirement $u_s' = u_B'$ then defines the remaining parameters of the model for which we obtain $S_n = 8$ Jy, $\nu_u = 3 \times 10^{16}$ Hz, $\Gamma = 14$, $n_1 = 9 \times 10^{-4}$ cm^{-3}, $B_1 = 1.5 \times 10^{-3}$ G, $\nu_b = 1.2 \times 10^{12}$ Hz, $R = 40$ pc, $L_{so} = L_{co} = 4 \times 10^{49}$ erg/s, $L_I = 2 \times 10^{50}$

erg/s. The Compton power emerges at hard X-ray and γ-ray energies. The total energy required in this model is $\sim 2 \times 10^{57}$ erg, comparable with the inferred radiant energy but ~ 30 times that directly observed.

In the second model, we assume that the steep optical spectrum is intrinsic so that $\nu_u = 3 \times 10^{13}$ Hz and in addition $S_n = 5$ Jy, $\nu_n = 17$ GHz, $\alpha_i = 0$ which are also compatible with radio observations. The remaining parameters are $\Gamma = 7$, $n_1 = 1.5 \times 10^{-1}$ cm^{-3}, $B_1 = 6 \times 10^{-3}$ G, $\nu_b = 3 \times 10^{11}$ Hz, $R = 9$ pc, $L_{so} = L_{co} = 2 \times 10^{48}$ erg/s, $L_I = 1 \times 10^{49}$ erg/s. In this version, the total energy supplied is $\sim 8 \times 10^{55}$ erg. (In fact, as discussed in the following section, it is possible to reduce the power requirements by a further factor $\gtrsim \Gamma^{-2}$ if the explosion is anisotropic.)

In both of these models, substantial X-ray and γ-ray fluxes are expected. In a SI radiative shock, the radio and optical fluxes reach their maximum values when the injection of energy ceases. The shock will subsequently decelerate to a mildly relativistic expansion speed before the radius increases by a quarter (see Paper I). A conventional non-relativistically expanding radio source will then evolve comparatively slowly with time, whilst the optical and infrared emission should decay very abruptly. If a similar outburst occurs again it will be especially interesting to know the *VLB* structure of the source. In the former model, the predicted source radius whilst it is radiating optically is $\theta \sim k_\theta k_o \Gamma C t_o / D \sim 0.2$ milliarcsec. However, after the injection of energy ceases, the observed angular size of the radio source should increase at a rate governed by light travel time effects to a maximum size $\theta \sim (1+z)^2 k_o \Gamma^2 C t_o / D \sim 5$ milliarcsec, evaluating Γ, t_o when the injection ceases. In the latter model, θ increases from ~ 0.1 to ~ 1 milliarcsec.

4.3 X-RAY INVERSE COMPTON RADIATION: CENTAURUS A

The nucleus of the radio galaxy Centaurus A (NGC 5128) has been observed from radio to extremely hard γ-ray energies, and variability on a timescale as short as a day has been claimed. It thus provides a good testing ground for theoretical models of active galactic nuclei. An accurate picture of the spectrum requires observations at widely different frequencies made within a few hours of each other. Such data are not as yet available and so our discussion must be based on measurements made at different epochs and is therefore quite approximate.

The radio spectrum indicates the presence of at least two separate components. Kellermann (1974) has found that the mm spectrum is self-absorbed at $\nu_n \sim 3 \times 10^{10}$ Hz and is possibly variable on a timescale of days. The radio luminosity is $\sim 10^{41}$ erg/s. There is a lower frequency radio component that we do not consider here. The X-ray spectrum extends from $\lesssim 3 \times 10^{17}$ Hz to $\gtrsim 3 \times 10^{21}$ Hz (Hall *et al.* 1976) with a spectral index ~ 0.75 (Stark, Davison & Culhane 1976; but see Mushotzky *et al.* 1976) and a luminosity $\gtrsim 10^{43}$ erg/s. Winkler & White (1975) found evidence for six-day variability at X-ray energies.

We confine our attention to a blast wave model that can explain both the mm and X-ray observations in which the X-ray photons are *twice* Compton-scattered radio photons. We again assume some potentially observable spectral parameters so that we can solve for the power and duration of the underlying explosion. If the mm spectrum cuts off at ~ 50 GHz and the X-ray spectrum at 10^{22} Hz, then $\gamma'_u \sim 700$. Combining equations (2), (10), (14), (26), (28) we obtain the solution $\beta \sim 0.5$, $B \sim 0.02$ G, $t_o \sim 3 \times 10^5$ s for an adiabatic SI ($k = 0$) model. Next, from equations (12), (34), (36) we obtain $n_1 \sim 2 \times 10^4$ cm^{-3}, $L_I \sim 10^{45}$ erg/s. These parameters characterize a self-consistent model in which the majority of the radiated power takes the form of hard X-ray photons, but for which the total radiative efficiency is only $\phi \sim 0.02$. There should be no break in either the mm or X-ray spectrum as $\gamma'_b > \gamma'_u$.

If this model is approximately correct then the mm and X-ray emission from Cen A should vary on a timescale of days and be correlated. Each outburst would be associated with an energy $\sim 3 \times 10^{50}$ erg. Grindlay (1975) has developed an alternative two-component model in which the hard X-rays are produced by a single Compton scattering of infrared photons. In this model, correlated 10 μm and MeV variation is predicted. In our model, the once-scattered radio photons will contribute a power $\sim 10^{42}$ erg/s to the visible band. However, because of the heavy observation of the nucleus, this is unlikely to be visible. A further prediction of our model is that the angular size at frequencies $\gtrsim 3 \times 10^{10}$ Hz be $\sim$ 3–10 milliarcsec.

Grindlay *et al.* (1975a, b) have also observed a variable γ-ray flux from Cen A with a luminosity $\gtrsim 10^{41}$ erg/s which is interpreted by Grindlay (1975) as Compton-scattered synchrotron soft X-rays. The simplest interpretation of these γ-ray photons in a blast wave model is that they result from Compton scattering of hard X-rays by relativistic electrons in the piston, with individual kinetic energies $\gtrsim 100$ GeV. For example, if the injection fluid contains protons and electrons moving with a bulk Lorentz factor ~ 100, then the electrons will only cool after passing through an inner shock, being given equipartition energies ~ 100 GeV (see Section 5).

5 Discussion

5.1 PRIME MOVERS

We have outlined the basic physics and application of a dynamically self-consistent model of a relativistically expanding Compton-synchrotron source. However, we have not as yet discussed the ultimate origin of the radiant energy associated with quasar and related outbursts. Existing models of galactic nuclei usually postulate either a succession of stellar-mass explosions (e.g. supernovae) or the presence of a massive object (e.g. superstar or black hole).

One possibility within the former category is that successive outbursts are associated with the formation of a rapidly spinning pulsar which slows down on a timescale $\sim$ months by the radiation of relativistic particles and strong waves (e.g. Arons, Kulsrud & Ostriker 1975). Alternatively, as envisaged by Colgate & Johnson (1960), an appreciable fraction of the energy released in a supernova can be converted into relativistic particles by means of a strong shock which accelerates outwards through the star's envelope. For an ER blast wave, the total energy of the explosion should greatly exceed the rest mass energy of the associated particles which in the case of strong waves requires that at least one hole be pierced through the stellar envelope.

However, as exemplified by AO 0235+164, the total energy associated with an outburst sometimes appears to exceed $1 M_{\odot} c^2$ and, at least for these cases, models involving massive objects seem more plausible. Undoubtedly the most natural mechanisms for relativistic energy release in this context involve some form of hydromagnetic or electromagnetic instability, and a variety of proposals have appeared in the literature (e.g. Piddington 1970; Ozernoi & Somov 1971; Sturrock & Barnes 1972; Pringle, Rees & Pacholczyk 1973). An attractive feature of this idea is that successive explosions can be focused along the same direction (the rotation axis) as some *VLB* observations seem to require. Shields & Wheeler (1976) have investigated the energetics of accretion disk models and point out that there may be a problem in storing enough energy in a disk to account for the outbursts, particularly if the total time-averaged power associated with the variable component greatly exceeds the integrated luminosity. (Their 'scenarios 1 and 2' correspond to A1 and SI outbursts in our terminology.) Only those blast wave models with fairly high radiative efficiency are likely to be acceptable in this context.

In general, these two possibilities can best be distinguished by detecting the presence or absence of motion of the centroid of radio emission using *VLB* techniques and deciding whether or not the energy per outburst is in any sense quantized at some fraction of a stellar rest mass. (Positive evidence for the latter would not necessarily rule out accretion models because the gas could be supplied by the tidal disruption of individual stars in the manner investigated by Hills 1975.)

In this paper we have investigated the hypothesis that the observed radiation is of a secondary nature associated with a strong shock rather than the explosion itself. This need not be the case. If the debris contains relativistic protons and electrons of large enough energy, then the electrons may also be able to radiate away their internal energy by the inverse Compton effect before they reach the expanding shock front. In the discussion of Cen A, we attributed the observed 300 GeV γ-rays to this effect. In fact, as discussed in Paper I, SI solutions for the shocked exterior medium can be joined onto solutions for the shocked interior medium within which proton–electron equipartition might be established. (In a similar explosion involving positrons and electrons very little of the explosion energy would be associated with the outer shock.) Alternatively, should the interior fluid be predominantly electromagnetic as it is in strong wave models, then we need not necessarily expect a large primary flux of high-energy photons.

There is of course no reason why inverse Compton and other radiative processes associated with the explosion cannot be responsible for either the steady or the variable component of the observed energy at optical and shorter wavelengths. However, unless coherent processes are involved, brightness temperature limitations ensure that the radio and infrared emissions must occur at radii $\gtrsim 10^{18}$ cm, 10^{14} cm, respectively which, on some models at least, exceeds the size of the initial explosion volume.

5.2 ANISOTROPIC BLAST WAVES

So far we have confined our attention to spherically symmetric blast waves, whereas the only direct evidence that we have concerning the geometry of outbursts in galactic nuclei comes from *VLBI* observations which can often (e.g. Cohen *et al.* 1976; Wittels *et al.* 1976) be interpreted in terms of two or three components separating with apparent linear speeds in excess of c. If the present calculations are to be applicable, then clearly either the energy supply or the external medium must be anisotropic. For instance, if the explosion occurs in a disk, then the momentum may be released parallel and antiparallel to the rotation axis (*cf.* Sturrock & Barnes 1972). Alternatively the explosion debris from an isotropic explosion could be focused if the surrounding medium took the form of a flattened cloud (e.g. Sanders 1976; Möllenhoff 1976).

The simplest relevant example of an anisotropic energy supply occurs when the momentum is released into two oppositely directed cones. In the ER case, the strong forward beaming of the radiation permits a significant simplification: if a large variation is observed and if the opening angle of the cone exceeds $1/\Gamma$, one may assume that the line of sight lies inside the cone. The observed spectrum is then unchanged, but the total luminosity and energy are reduced by $\Omega/4\pi$, where Ω is the solid angle subtended by the two cones. This is particularly important in the case of a source like AO 0235 +164, for which the total energy estimates are large.

There are two approximate techniques for handling the propagation of non-relativistic shock waves in non-uniform media. Kompaneets (1960) modelled his treatment on the Sedov similarity solution, assuming that all the swept-up material is concentrated into a thin shell that is pushed out by an isobaric internal fluid. In an alternative treatment, Lambauch

& Probstein (1969) assumed that the flow is locally radial and that each portion of the shock behaves as an independent segment of a spherical explosion. This latter approach is definitely more appropriate to the ER case and the results of Section 2 can be straightforwardly modified to apply to it. However, the total energy requirements are not significantly reduced unless the energy supply is anisotropic.

5.3 THE EXTERNAL MEDIUM

We have also not discussed the nature of the external medium through which the shock is driven. Again there are some potential difficulties, the foremost amongst them being that if successive explosions are not spatially separated and the interval between them is short, then the external medium may not be able to recover sufficiently rapidly for the assumptions we have made to be valid. This need not be a problem if, for instance, a galactic nucleus is permeated by a filamentary emission-line region, rather like the Crab Nebula. With a large filling factor, the average filament separation could be sufficiently small for the intervening medium to be refilled between explosions in which case the duration of an impulsive outburst should decrease with the time that has elapsed since the previous one. In the absence of filaments, the medium will become uniform again after a time comparable with the sound travel time across the volume enclosed by the shock when it has become weak.

If the surrounding material is in the form of a wind, we have thus far assumed that it is non-relativistic and has a uniform velocity, so that $\rho_1 \propto R^{-2}$. This density law will still be obeyed by a relativistic wind, but it will no longer be adequate to ignore its motion. If it has a Lorentz factor $\gamma_{\rm wind}$, then the mean electron energy behind the shock will satisfy equation (9) with

$$k_\gamma = 0.33\left(1-\frac{\beta_{\rm wind}}{\beta}\right)^2 \quad \mathrm{NR}\,(\beta \ll 1)$$
$$= \frac{k_w}{\sqrt{2}(1+\beta_{\rm wind})\gamma_{\rm wind}} \quad \mathrm{ER}\,(\Gamma \gg 1). \tag{49}$$

This possibility is particularly interesting in the context of relativistically expanding compact radio sources for which high bulk Lorentz factors are required in conjunction with small values of $\bar{\gamma}'_e$.

Several other situations can be described by modifications of the theory outlined in Section 2. Two examples that we have not considered are the illumination of a standing shock in an outflow by a sudden increase in the energy flux, and the driving of strong shocks into the filaments themselves.

6 Conclusions

In this paper we have attempted to describe a general dynamical theory of outbursts in active galactic nuclei based on the synchrotron and Compton emission of relativistic electrons accelerated behind an expanding shock. There are three outstanding theoretical deficiencies: the treatment of particle acceleration is *ad hoc*, possible amplification of magnetic field and its dynamical effect is ignored and only spherical (or quasi-spherical) geometries are considered. Nevertheless we have demonstrated that it is possible to account for observations in several wavebands self-consistently, without requiring completely unacceptable quantities of unseen energy.

In the examples discussed in the preceding two sections, we have undoubtedly overinterpreted the observational data in order to deduce unique sets of source parameters. As emphasized by earlier authors (e.g. BJO), simultaneous *VLB*, mm and X-ray observations of radio and optical outbursts are needed to overspecify, and thus test the simple models. The discovery of spectral breaks at mm or X-ray frequencies would be of special importance. In addition, if the pistons contain relativistic electrons the inverse Compton scattered γ-rays are to be expected from some of the strongest sources, although this cannot be directly quantified.

Typical radio variables, exemplified by 3C120, can be accounted for by mildly relativistic blast waves in which GeV electrons are automatically accelerated behind the shock. A wide variety of spectral behaviour can be reproduced by simple models which can be fairly efficient in the sense that they do not invoke much more energy, either at shorter wavelengths or in an unseen dynamical form, than is directly observed. This means that the majority of such outbursts *could* be accounted for by means of stellar-mass objects. The comparatively rare low-frequency variables like CTA102 require extremely relativistic expansion and have much larger energy requirements, typically $\gtrsim 10^4$ times that directly observed (*cf.* BJO). Unless there is evidence for associated high-frequency variability, it seems more probable that the explanation for low-frequency fluctuation lies elsewhere. As with the Sun, it would be surprising if one explanation sufficed to account for all radio activity.

Optical and X-ray variation can be similarly analysed and attributed either to synchrotron radiation from ER shocks (as in AO0235+164) or inverse Compton radiation (as in Cen A) from mildly relativistic explosions. It is unlikely that powerful optical outbursts can be derived from stellar-mass objects unless they are extremely anisotropic. Nevertheless it seems to be possible to derive self-consistent models that predict a ratio of unobserved to observed energy of order unity.

If future observations can be generally interpreted in this manner then, by understanding the secondary processes responsible for non-thermal activity in quasars, it should be possible to place important constraints on the nature of the primary energy source.

Acknowledgments

RDB gratefully acknowledges support by a Parisot Fellowship at Berkeley, a research fellowship at St John's College, Cambridge, and partial support at Caltech under the National Science Foundation [AST75-01398 AO1]. CFM was supported in part by NSF grant AST75-02181. We thank J. Arons, A. Fabian, G. Field, and M. Rees for helpful discussions and encouragement.

References

Altschuler, P. R. & Wardle, J. F. C., 1976. *Mem. R. astr. Soc.*, **82**, 1.
Arons, J., Kulsrud, R. M. & Ostriker, J. P., 1975. *Astrophys. J.*, **198**, 687.
Blandford R. D. & McKee, C. F., 1976. *Phys. Fluids*, **19**, 1130.
Burbidge, G. R., Jones, T. W. & O'Dell, S. L., 1974. *Astrophys. J.*, **193**, 43.
Castor, J., McCray, R. & Weaver, R., 1975. *Astrophys. J. Lett.*, **200**, L107.
Cohen, M. H., 1975. Proc. Seventh Texas Symp., Relativistic astrophysics, *Ann. N. Y. Acad. Sci.*, **262**, 428.
Cohen, M. H., Moffet, A., Romney, J. D., Schilizzi, R. T., Seielstad, G. A., Kellermann, K. I., Purcell, G. H., Shaffer, D. B., Pauliny-Toth, I. I. K., Preuss, E., Witzel, A. & Rinehart, R., 1976. *Astrophys. J. Lett.*, **206**, L1.
Colgate, S. A., Colvin, J. D. & Petschek, A. G., 1975. *Astrophys. J. Lett.*, **197**, L105.

Colgate, S. A. & Johnson, M. H., 1960. *Phys. Rev. Lett.*, **5**, 235.
Condon, J. J. & Dressel, L. L., 1973. *Astrophys. Lett.*, **15**, 203.
Cotton, W. D., 1976. *Astrophys. J. Lett.*, **204**, L63.
de Bruyn, A. G., 1976. *Astr. Astrophys.*, in press.
Demoulin, M.-H. & Burbidge, G. R., 1968. *Astrophys. J.*, **154**, 3.
Dent, W. A., 1968. *Astrophys. J. Lett.*, **153**, L29.
Grindlay, J. E., 1975. *Astrophys. J.*, **199**, 49.
Grindlay, J. E., Helmken, M. F., Hanbury-Brown, R., Davis, J. & Allen, L. R., 1975a. *Astrophys. J. Lett.*, **197**, L9.
Grindlay, J. E., Schnoppen, H., Schreier, E. J., Gursky, H. & Parsignault, D. R., 1975b. *Astrophys. J. Lett.*, **201**, L133.
Hall, R. D., Meegan, C. A., Walraven, G. D., Djuth, F. T. & Haymes, R. C., 1976. *Astrophys. J.*, **210**, 631.
Hills, J. G., 1975. *Nature*, **254**, 295.
Hirasawa, J. & Tabara, M., 1970. *Astrophys. Lett.*, **7**, 121.
Hoyle, F., Burbidge, G. R. & Sargent, W. L. W., 1966. *Nature*, **209**, 751.
Hunstead, R. W., 1972. *Astrophys. Lett.*, **12**, 193.
Jones, T. W., O'Dell, S. L. & Stein, W. A., 1974. *Astrophys. J.*, **188**, 353.
Jones, T. W. & Tobin, W., 1977. *Astrophys. J.*, submitted.
Katz, J. I., 1976. *Astrophys. J.*, **206**, 910.
Kellermann, K. I., 1974. *Astrophys. J. Lett.*, **194**, L135.
Kellermann, K. I., Clark, B. G., Jauncey, D. L., Broderick, J. J., Shaffer, D. B., Cohen, M. H. & Niell, A. E., 1973. *Astrophys. J.*, **183**, L51.
Kellermann, K. I. & Pauliny-Toth, I. I. K., 1969. *Astrophys. J. Lett.*, **155**, L71.
Kinman, T. D., 1968. *Astr. J.*, **73**, 885.
Kompaneets, A. S., 1960. *Sov. Phys. Dokl.*, **5**, 46.
Lambauch, D. D. & Probstein, P. F., 1969. *J. Fluid Mech.*, **35**, 53.
Landau, L. D. & Lifshitz, E. M., 1959. *Fluid mechanics*, Pergamon, Oxford.
Ledden, J. E., Aller, H. D. & Dent, W. A., 1976. *Nature*, **260**, 752.
Locke, J. L., Andrew, B. H. & Medd, W. J., 1969. *Astrophys. J. Lett.*, **157**, L81.
McKee, C. F., 1971. *Phys. Fluids*, **14**, 2164.
McKee, C. F., 1974. *Astrophys. J.*, **188**, 335.
MacLeod, J. M., Andrew, B. H. & Harvey, G. A., 1976. *Nature*, **260**, 751.
Medd, W. J., Andrew, B. H., Harvey, G. A. & Locke, J. L., 1972. *Mem. R. astr. Soc.*, **77**, 109.
Möllenhoff, C., 1976. *Astr. Astrophys.*, **50**, 105.
Mushotzky, R. F., Baity, W. A., Wheaton, W. A. & Peterson, L. E., 1976. *Astrophys. J. Lett.*, **206**, L45.
O'Connell, P. F. ed., 1971. *Nuclei of galaxies*, Pontifical Academy of Sciences, Rome.
Oke, J. B., Neugebauer, G. & Becklin, E. E., 1970. *Astrophys. J.*, **159**, 341.
Ozernoi, L. M. & Sazonov, V. N., 1969. *Astrophys. Sp. Sci.*, **3**, 395.
Ozernoi, L. M. & Somov, B. V., 1971. *Astrophys. Sp. Sci.*, **11**, 264.
Pacholczyk, A. G., 1970. *Radio astrophysics*, W. H. Freeman & Co., San Francisco.
Pauliny-Toth, I. I. K. & Kellermann, K. I., 1966. *Astrophys. J.*, **146**, 634.
Pauliny-Toth, I. I. K. & Kellermann, K. I., 1968. *Astrophys. J. Lett.*, **152**, L169.
Peterson, F. W. & Dent, W. A., 1973. *Astrophys. J.*, **186**, 421.
Peterson, F. W. & King, C., 1975. *Astrophys. J.*, **195**, 753.
Piddington, J. H., 1970. *Mon. Not. R. astr. Soc.*, **148**, 131.
Pringle, J. E., Rees, M. J. & Pacholczyk, A. G., 1973. *Astr. Astrophys.*, **29**, 179.
Rees, M. J., 1966. *Nature*, **211**, 468.
Rees, M. J., 1967a. *Mon. Not. R. astr. Soc.*, **135**, 345.
Rees, M. J., 1976b. *Mon. Not. R. astr. Soc.*, **137**, 429.
Rees, M. J. & Simon, M., 1968. *Astrophys. J. Lett.*, **152**, L145.
Rieke, G. M., Grasdalen, G. L., Kinman, T. D., Hintzen, P., Wills, B. J. & Wills, D., 1976. *Nature*, **260**, 754.
Sanders, R. M., 1976. *Astrophys. J.*, **205**, 335.
Seielstad, G. A., 1974. *Astrophys. J.*, **193**, 55.
Shields, G. A. & Wheeler, J. C., 1976. *Astrophys. Lett.*, **17**, 69.
Shklovsky, I. S., 1960. *Sov. Astr. A. J.*, **4**, 243.
Stark, J. P., Davison, P. J. N. & Culhane, J. L., 1976. *Mon. Not. R. astr. Soc.*, **174**, 35P.
Sturrock, P. A. & Barnes, C., 1972. *Astrophys. J.*, **176**, 31.
Usher, P. D., 1972. *Astrophys. J. Lett.*, **172**, L25.

van der Laan, H., 1966. *Nature*, **211**, 1131.
Visvanathan, N., 1973. *Astrophys. J.*, **179**, 1.
Winkler, P. F. & White, A. E., 1975. *Astrophys. J. Lett.*, **199**, L139.
Wittels, J. J., Cotton, W. D., Counselman, C. C., Shapiro, I. I., Hinteregger, H. F., Knight, C. A., Rogers, A. E. E., Whitney, A. R., Clark, T. A., Hutton, L. K., Rönnäng, B. O., Rydbeck, O. E. H. & Niell, A. E., 1976. *Astrophys. J. Lett.*, **206**, L75.
Woltjer, L., 1972. *A. Rev. Astr. Astrophys.*, **10**, 129.

Appendix: evaluation of constants

The constants introduced in the text are listed in Tables 6 and 7 with their definitions and values in both the NR and ER limits. In this Appendix we outline the evaluation of some of these constants for different types of blast wave. For simplicity, we ignore cosmological factors which are included in the tables.

First consider the factors f (equation 17) and g (equation 19). For a Maxwellian, $f = 1.33$ and $g = k_{\rm thn} f = 0.019$. For a power law extending from γ_l' to γ_u' (i.e. there is no break in the distribution $-\gamma_u' \ll \gamma_b'$)

$$f = \begin{cases} \dfrac{\gamma_u'}{\bar{\gamma}_e'} \dfrac{\psi_3}{\psi_2} & 1 < s \leqslant 2 \\ \left(\dfrac{\gamma_u'}{\bar{\gamma}_e'}\right)^{3-s} \dfrac{\psi_3 \psi_1^{s-2}}{\psi_2^{s-1}} & 2 \leqslant s < 3 \end{cases}$$

$$g = \begin{cases} k_{\rm thn} \left(\dfrac{\bar{\gamma}_e'}{\gamma_u'}\right)^{2-s} \dfrac{\psi_3}{\psi_2} & 1 < s \leqslant 2 \\ k_{\rm thn} \dfrac{\psi_3 \psi_1^{s-2}}{\psi_2^{s-1}} & 2 \leqslant s < 3 \end{cases} \qquad \text{(A1)}$$

Table 5. Definition of physical variables.

$\Gamma \equiv (1-\beta^2)^{-1/2}$	Shock Lorentz factor
R	Shock radius
$t^{\star}$	Time
w†	Enthalpy
ρ†	Rest mass density
n†‡	Electron density
B†‡	Magnetic flux density
$b^{\star\star}$	$8\pi\rho_1 c^2/B_1^2$
D	Luminosity distance
S_ν	Observed flux density
$L^{\star}$‡§	Luminosity (sum of emitted powers)
$\bar{\gamma}_e'$	Mean electron Lorentz factor in comoving frame behind shock
γ_l', γ_u'	Limits of electron distribution function
$\bar{\nu}$‡	Peak frequency radiated by electron of energy $\bar{\gamma}_e' m_e c^2$
C	$\bar{\nu}'/\gamma_e'^2 B'$
$f^{\star\star}$	$\langle\gamma_e'^2\rangle/\bar{\gamma}_e'^2$
$g^{\star\star}$	$k_{\rm thn} f(\bar{\gamma}_e'/\gamma_u')^{2(1-\alpha)}$
u'§	Energy density measured in comoving frame

* A subscript o indicates a quantity measured by a distant observer.
† A subscript 1 indicates a quantity measured in the unshocked external medium.
‡ A superscript $'$ indicates a quantity measured in the comoving frame behind the shock. Unprimed quantities are measured in the frame of the external medium.
§ Subscripts B, S, C, refer to the magnetic, synchrotron and Compton components respectively.
** Unlike the k factors, the quantities b, f, g are not necessarily close to unity; for typical examples, however, $0.1 \lesssim f, g \lesssim 10$.

Table 6. k factors: definition and evaluation in NR and ER limits.

k_x ★	Definition	NR	ER
k_σ ‡	E or $L_1 t\Gamma^{-2} = k_\sigma w_1 \Gamma^2 \beta^2 V$	Table 7	
k_e	Electron fraction of post-shock internal energy	Assumed to be ~ 0.5	
k_w	$w_1 = k_w \rho_1 c^2$	1	$\gtrsim 1$
k_B †	$B'_2 = 4k_B \Gamma B_1$	1	0.71
k_R	$R = k_R \beta c t$	Table 1	1
k_o	$R = k_o \Gamma^2 \beta c t_o$	$k_R (1+z)^{-1}$	$2(m+1)(1+z)^{-1}$
k_θ	$\theta = k_\theta R \Gamma^{-1} D^{-1}$	$(1+z)^2$	$(1+z)^2(m+2)^{[(m+2)/2(m+1)]}$
k_γ ‡	$(\gamma_2 k_w - 1) = k_\gamma \Gamma \beta^2$	0.33	$0.71 k_w$
k_ν	$\nu = k_\nu \Gamma \nu'$	$(1+z)^{-1}$	$1.4(1+z)^{-1}$
k_{thk}	$S_\nu = k_{thk} \cdot 2\left(\frac{\gamma'_{eff} m_e c^2}{3}\right)\left(\frac{\nu'}{c}\right)^2\left(\frac{\nu}{\nu'}\right)\frac{\pi R^2}{D^2}$	M: $(1+z)^2$	Table 7
		PL: $(1+z)^2 k_{B_\nu}$	Table 7
k_{thn}	$S_\nu = k_{thn} \frac{L_{so}}{4\pi D^2}\left(\frac{\nu}{\nu_u}\right)^{-\alpha}\frac{(1-\alpha)}{\nu_u}$	M: 0.014	
		PL: Table 8	
k_{B_ν}	$B'_{\nu'} = k_{B_\nu} \cdot 2\left(\frac{\gamma'_{eff} m_e c^2}{3}\right)\left(\frac{\nu'}{c}\right)^2$	M: 1	
		PL: Table 8	
k_L	$L_o = k_L \Gamma^2 L'$	1	Table 7
k_P ‡	$L'_s = k_P \cdot \frac{4\pi}{3} R^3 n_1 \cdot \frac{4}{3}\sigma_T c \bar{\gamma}'^2_e f u'_B$		Table 7
k_u	$2\pi R^2 c u' = k_u k_L L'$		$\sim \frac{1}{4} \ln(10R/\Delta R)$
k_ϕ	$\phi = k_\phi \phi_s (3b\phi_s/b_{crit})^i$		$1 \leqslant k_\phi \leqslant 3$

★ n.b. k is the exponent in the expression $n_1 \propto r^{-k}$.
† k_B is calculated assuming that the only field amplification is due to compression of magnetic flux.
‡ k_σ, k_γ, k_P are calculated in the NR limit using the similarity solutions discussed in Paper I, assuming an effective specific heat ratio of 13/9 corresponding to a single temperature ER electron–NR proton plasma ($k_e = 2/3$), and $k_w = 1$.

Table 7. k factors.

Explosion		Adiabatic impulsive		Steady injection	
Medium		Uniform ($k=0$)	Wind ($k=2$)	Uniform ($k=0$)	Wind ($k=2$)
k_σ(NR)		1.2	1.7	2.2	7.5
k_σ(ER)		0.35	0.67	2.0	5.4
k_P(NR)		0.39	1.2	2.0	3.0
k_P(ER)		0.21	0.43	0.74	2.1
k_L(ER)		5.9	14	0.70	2.0
k_{thk}(ER)	M	$0.35(1+z)^2$	$0.41(1+z)^2$	$0.41(1+z)^2$	$0.45(1+z)^2$
	PL	$0.26 k_{B_\nu}(1+z)^2$	$0.34 k_{B_\nu}(1+z)^2$	$0.37 k_{B_\nu}(1+z)^2$	$0.43 k_{B_\nu}(1+z)^2$

where

$$\psi_n = \frac{1}{|s-n|}\left[1 - \left(\frac{\gamma'_e}{\gamma'_u}\right)^{|s-n|}\right] \qquad s \neq n$$

$$= \ln(\gamma'_u/\gamma'_e), \qquad s = n.$$

and where $\bar{\gamma}'_e$ is the average energy per electron just behind the shock. Note that in the definitions of f and g we are treating the relativistic electron distribution functions ($dn/d\gamma'_e$) and magnetic field strength as homogeneous in the emitting region. This ignores some uncertain correction factors of order unity that cannot be calculated satisfactorily without making additional assumptions.

If there is a break in $dn/d\gamma'_e$, the results of Section 2.3 must be generalized. Provided that $\gamma'_1 \ll \gamma'_b \ll \gamma'_u$, equations (15) and (19) are still valid if f is re-defined as

$$f = \begin{cases} \dfrac{\gamma'_b}{\gamma'_e} & 1 < s_i < 2 \\ \left(\dfrac{\bar{\gamma}'_e}{\gamma'_b}\right)^{3-s_i} \dfrac{\psi_1^{s_i-2}\psi_3}{\psi_2^{s_i-2}} & 2 < s_i < 3. \end{cases} \tag{A2}$$

In equation (19) it is adequate to use the value of g defined in equation (A1) for $\nu \leqslant \nu_b$ and multiply the expression for the flux by $(\nu_b/\nu)^{1/2}$ for $\nu \geqslant \nu_b$. Equation (15) must be modified similarly.

Secondly, we consider the constant k_u (equation (20)). For a nonrelativistic uniform, thin shell of radius R and thickness ΔR, we find that at a point in the shell labelled by $\chi = (R - r)/\Delta R$

$$k_u = \tfrac{1}{4}\ln\left(\frac{5.44R}{\Delta R\chi^{\chi}(1-\chi)^{(1-\chi)}}\right)$$

For example, at a point halfway through the shell ($\chi = \tfrac{1}{2}$) $k_u = 1.2$ for $R/\Delta R = 10$. For a strongly radiative shock k_u can become as large as 3. A similar expression seems to hold for relativistic shocks. In the text, we use $k_u = 2 - 3$.

Next we evaluate several of the k factors for both adiabatic impulsive (AI) and non-radiative, steady energy injection (SI), extreme relativistic blast waves. The time at the source t is related to observer time t_o by

$$t = t_o + r\mu/c \tag{A3}$$

where $\mu = \cos\theta$ and r, θ are spherical coordinates centred at the site of the explosion or energy generation. For a fixed value of observer time, the maximum value of t is

$$t_m = t_o + R_m/c \tag{A4}$$

where $R_m \equiv R(t_m)$ is the radius of the shock. (In the text, the subscript m is omitted for simplicity.) Following the notation of Paper I, we introduce the variable

$$\chi = 2(m+1)\,\Gamma^2(1 - r/ct) \tag{A5}$$

where

$$\Gamma^2 = \Gamma_m^2\,\tau^{-m} \tag{A6}$$

$\tau = t/t_m$, and we have omitted a term $O(\Gamma^{-2})$ relative to the term retained in the expression for χ. The quantity χ equals unity at the shock front and increases to $\chi_c \sim 2$ for SI blast waves or to a value $O(\Gamma^2) \gg 1$ for AI blast waves. The pressure, Lorentz factor, and density, n measured in the fixed frame (denoted by n' in Paper I) of the shocked fluid can be expressed

$$p' = \tfrac{2}{3}\,w_1\,\Gamma^2 f(\chi) \tag{A7}$$

$$\gamma^2 = \tfrac{1}{2}\Gamma^2 g(\chi) \tag{A8}$$

$$n = 2n_1\Gamma^2 h(\chi) \tag{A9}$$

where f, g, and h are all normalized to unity at $\chi = 1$. The ambient density n_1 is assumed to vary as r^{-k}, so that n can be written as $2n_{1m}\Gamma_m^2\tau^{-(m+k)}h(\chi)$. The synchrotron power P radiated by a single electron with energy $\bar{\gamma}_e' m_e c^2$ can be written $P = P_m \tau^{-2m-k} f^2$, where we have taken $b = 8\pi\rho_1 c^2/B_1^2$ to be constant.

The factor k_P introduced in equation (17) is readily found to be

$$k_P = \frac{3}{m+1}\int d\chi h f^2 \left(\frac{n_1}{n_1^*}\right) \tag{A10}$$

where n_1^* is the external density when the fluid element was shocked. For AI blast waves, m and k are related by $m = 3 - k$, the solution presented in Paper I yields

$$k_P = \frac{9}{43 - 8k}. \qquad \text{(AI)} \tag{A11}$$

The requirement that the mass swept up by the blast wave be finite implies $k < 3$ so that $k_P < 0.9$. An exact analytic result is not obtainable for SI blast waves, but the results of Paper I indicate that $m = 1 - \tfrac{1}{2}k$, $g \sim 1$, $\bar{h} = \tfrac{1}{2}(4-k)/(3-k)\,(\chi_c - 1)$, and $\bar{f}^2 \sim 0.7$, so that $k_P \sim 2.1/(3-k)$.

To evaluate the constant k_L relating the observed and the emitted luminosities (equation (16)), it is convenient to introduce the variable

$$\xi = 1 - (1-\mu)\,t/t_o. \tag{A12}$$

At $\mu = 1$, one has $\xi = 1$; one can show that $\xi = 0$ at $\mu = 0$ and ξ is small and negative at $\mu = -1$. In the extreme relativistic limit ($t \gg t_o$) one has

$$\tau^{m+1} = \xi/\chi, \tag{A13}$$

so that $\xi = \tau^{m+1}$ describes the outer surface of the blast wave at a fixed value of t_o. The observed luminosity is given in terms of the emissivity per steradian j measured in the observer's frame by

$$L_o = \int 4\pi j\, 2\pi r^2\, dr\, d\mu.|_{t_o = \text{constant}}. \tag{A14}$$

Since j/ν^3 is Lorentz invariant and since $j' = n'P/4\pi$, we have

$$4\pi j = n'P = \frac{\Gamma_m^6 \tau^3}{\gamma^3 \mathscr{D}^3} \tag{A15}$$

where

$$2(m+1)\,\mathscr{D} = 1 + \left[\frac{2(m+1)}{g\chi} - 1\right]\xi. \tag{A16}$$

Then we obtain $L_o = k_L \Gamma_m^2 L_m'$, where

$$k_L = \frac{6}{k_P(m+1)^2}\int_0^1 d\xi\, \xi^{(s-m-2k)/(m+1)} \int_1^{\chi_c} d\chi \frac{hf^2}{\mathscr{D}^3 g^2}\, \chi^{-[(6-2k)/(m+1)]} \tag{A17}$$

and in which χ_c is to be set equal to ∞ for the AI case.

For the AI case, $g\chi = 1$ (see Paper I) and we calculate $k_L = 5.9, 14$ for $k = 0, 2$ respectively. For the SI case, we again approximate g by 1 and treat hf^2 as constant to obtain $k_L \sim 0.70, 2.0$ again for $k = 0, 2$. Note that k_L generally exceeds unity because radiation is observed emitted prior to t_m; under the assumption that b is constant, we have $L' \propto t^{-3}$ (AI) and $L \propto t^{1-k}$ (SI). The rapid increase in L' with decreasing t accounts for the relatively large values of k_L in the AI case.

We next turn to the spectrum of the observed radiation. This too can be calculated approximately if we make enough simplifying assumptions. At sufficiently low frequencies, the synchrotron emission is optically thick and the radiation is emitted by a relativistically expanding surface. The observed flux is given by

$$S_\nu = \frac{1}{D^2}\int dA\, B'_{\nu'}\,(\nu/\nu')^3 \tag{A18}$$

where B'_ν is the source function and dA is an element of area projected onto the plane of the sky at fixed observer time, t_0. Generalizing Rees' (1967a) argument to the case of a time-varying Lorentz factor, $\Gamma^2 \propto t^{-m}$, we find that the element of area is

$$dA = \frac{2\pi c^2 t_m t_o}{(m+1)}\,\xi^{-[m/(m+1)]}\,[(m+2)\xi - 1]\,d\xi \tag{A19}$$

in the ER limit, where we have again taken $t \gg t_0$. The visible part of the surface extends from $\xi = 1$ to $\xi = 1/(m+2)$. For a Maxwellian distribution, $B'_{\nu'} = 2(\tilde{\gamma}'_e m_e c^2/3)\,\nu'^2/c^2$ and so the factor k_{thk} in equation (13) is given by

$$k_{thk}(m) = \frac{4}{(m+1)}\int_{1/(m+2)}^{1} d\xi\,\xi^{[(1-m)/(m+1)]}\left(\frac{(m+2)\xi - 1}{1+2(m+1)\xi}\right) \tag{A20}$$

For a power law distribution,

$$B'_{\nu'} = k_{B_\nu}\cdot 2\cdot \tfrac{1}{3}\left(\frac{\nu'}{CB'}\right)^{1/2} m_e \nu'^2, \tag{A21}$$

where k_{B_ν} depends on the spectral index α through the constants c_5, c_6 tabulated by Pacholczyk (1970)

$$k_{B_\nu(\alpha)} = 3.2\times 10^{-18}\,[c_5(2\alpha+1)]/[c_6(2\alpha+1)] \tag{A22}$$

k_{thk} is then given by

$$k_{thk} = [2/(m+1)]^{3/2}\,k_{B_\nu}\int_{1/(m+2)}^{1} d\xi\,\xi^{[2-2m+k]/[4(m+1)]}[(m+2)\xi - 1]/[1+(2m+1)\xi]^{1/2}. \tag{A23}$$

At higher frequencies, where the spectrum is optically thin, we can approximate the flux using the accurate expression for the observed luminosity involving k_L (equation (A17)) and assuming that it all originates at time t_m. For a Maxwellian distribution, $k_{thn} = 0.014$ as defined by equation (15). For a power-law distribution, a straightforward calculation gives

$$k_{thn} = \frac{9\sqrt{3}}{8\pi}(0.14)^{(3-s)/2}\left(\frac{s+7/3}{s+1}\right)\Gamma\left(\frac{3s-1}{12}\right)\Gamma\left(\frac{3s+7}{12}\right);\quad \tfrac{1}{3} < s < 3. \tag{A24}$$

Sample values of k_{B_ν}, k_{thk} and k_{thn} are given in Tables 7 and 8.

For frequencies $\nu > \nu_u(t_m)$ the observed flux will be dominated by contributions from

Table 8. Evaluation of k_{B_ν}, $k_{\rm thn}$ for power-law distribution functions.

s	1	1.5	2	2.5
α	0	0.25	0.5	0.75
k_{B_ν}	1.34	0.75	0.51	0.39
$k_{\rm thn}$	0.94	0.73	0.68	0.79

earlier times, and a 'global' power law can be produced. If we define a spectral function $F(\nu';\xi,\chi)$ by

$$4\pi j'_{\nu'} = n' P F(\nu';\xi,\chi),$$

normalized so that

$$\int F(\nu';\xi,\chi)\,d\nu' = 1, \tag{A25}$$

then the observed flux is given formally by

$$S_\nu = \frac{L'_{\rm m}}{4\pi D^2 k_P}\cdot\frac{3\sqrt{2}\Gamma_{\rm m}}{(m+1)^2}\int_0^1 d\xi\int_1^{\chi_{\rm c}}\frac{d\chi}{\chi}\,\frac{hf^2}{g^{3/2}\mathscr{D}^2}\,F(\nu';\xi,\chi)\left(\frac{\xi}{\chi}\right)^{[8-3m]/[2(m+1)]} \tag{A26}$$

For a Maxwellian distribution, F can be approximated by a δ function, $F=\delta(\nu'-\bar\nu')$. If we use the relation between the emitted frequency, ν' and the local mean critical frequency, $\bar\nu'$, we obtain

$$\frac{\nu'}{\bar\nu'} = \left(\frac{\nu}{\bar\nu_{\rm m}}\right)\frac{\mathscr{D}h}{f^2}\left(\frac{\xi}{\chi}\right)^{(m-1)/(m+1)} \tag{A27}$$

For the simplest example of an AI explosion in a uniform medium,

$$S_\nu = \frac{L'_{\rm o}}{4\pi D^2 k_{\rm L} k_P \bar\nu_{\rm m}}\cdot\frac{2^{17}\cdot 9}{29}\left(\frac{\bar\nu_{\rm m}}{\nu}\right)^4. \quad \nu \gtrsim 20\bar\nu_{\rm m}. \tag{A28}$$

The spectrum will be substantially curved in the range $\bar\nu_{\rm m} \lesssim \nu \lesssim 20\bar\nu_{\rm m}$. Analogous spectra can be calculated for power law distributions but these of course depend on the variation of ν'_u with time.